https://doi.org/10.5194/esd-2019-47
Preprint. Discussion started: 2 September 2019


Earth System Dynamics Discussions
Open Access
EGU

# Long-term Variances of Heavy Precipitation across Central Europe using a Large Ensemble of Regional Climate Model Simulations

Florian Ehmele[1], Lisa–Ann Kautz[1], Hendrik Feldmann[1], and Joaquim G. Pinto[1]

[1]Institute of Meteorology and Climate Research, Department Troposphere Research (IMK–TRO), Karlsruhe Institute of Technology (KIT), Hermann–von–Helmholtz–Platz 1, 76344 Eggenstein–Leopoldshafen, Germany.

**Correspondence:** Florian Ehmele (florian.ehmele@kit.edu)

**Abstract.** Widespread flooding events are among the major natural hazards in Central Europe. Such events are usually related to intensive, long-lasting precipitation. Despite some prominent floods during the last three decades (e. g. 1997, 1999, 2002, and 2013), extreme floods are rare and associated with estimated long return periods of more than 100 years. To assess the associated risks of such extreme events, reliable statistics of precipitation and discharge are required. Comprehensive observations, however, are mainly available for the last 50–60 years or less. This shortcoming can be reduced using stochastic data sets. One possibility towards this aim is to consider climate model data or extended reanalyses.

This study presents and discusses a validation of different century-long data sets, a large ensemble of decadal hindcasts, and also projections for the upcoming decade. Global reanalysis for the 20th century with a horizontal resolution of more than 100 km have been dynamically downscaled with a regional climate model (COSMO–CLM) towards a higher resolution of 25 km. The new data sets are first filtered using a dry–day adjustment. The simulations show a good agreement with observations for both statistical distributions and time series. Differences mainly appear in areas with sparse observation data. The temporal evolution during the past 60 years is well captured. The results reveal some long-term variability with phases of increased and decreased heavy precipitation. The overall trend varies between the investigation areas but is significant. The projections for the upcoming decade show ongoing tendencies with increased precipitation for upper percentiles. The presented RCM ensemble not only allows for more robust statistics in general, in particular it is suitable for a better estimation of extreme values.

## 1 Introduction

Ongoing climate change affects not only the global scale but also impacts the regional climate. Regarding air temperature, there is a more or less clear trend in the recent past, which reveals a clear anthropogenic signal. However, various climate simulations show distinct spatial differences for precipitation trends especially for heavy precipitation (e. g. Moberg et al., 2006; Zolina et al., 2008; Toreti et al., 2010). What is known is a theoretical increase of the water vapor capacity according to the Clausius–Clapeyron (CC) equation of about 6–7 % per degree of temperature increase (e. g. Trenberth et al., 2003; Berg et al., 2009). For instance, Lenderink et al. (2011), Berg et al. (2013), or O'Gorman (2015) showed that this CC rate can be surpassed up to a factor 2 (Super–Clausius–Clapeyron scaling). In contrast, Stephens and Ellis (2008) found a change of precipitation below the

https://doi.org/10.5194/esd-2019-47
Preprint. Discussion started: 2 September 2019


Earth System Dynamics Discussions

theoretical CC rate. Nevertheless, the CC rate generally thought to be a good proxy for future precipitation projections (Westra et al., 2013).

Easterling et al. (2000) showed that a linear trend in heavy precipitation varies for different countries and depends also on the considered time period. Moberg and Jones (2005) evaluated observational data from about 80 rain gauges in central and western Europe for the time period 1901–1999 revealing an increase in extreme winter precipitation. A recent review of observed variability and trends in extreme climate events states that it is difficult to find significant relations between the greenhouse gas-enhanced climate change and increases or decreases in extreme precipitation events (Field et al., 2012). This is attributed to their rare occurrence, the general high spatial variability of precipitation, and due to a lack of long-term high-quality observations. Feldmann et al. (2013) found an increase of both areal mean precipitation and extremes in central Europe in order of 5–10 % which will continue with almost same magnitude for the next decades. Moreover, the use of high resolution regional climate models (RCM) instead of global data sets revealed a more detailed and orographically related spatial structure of the precipitation fields and trends. Global tendencies towards more intense precipitation throughout the 20th century were also revealed by Donat et al. (2016).

In summary, these studies partly document contrasting results. Following Field et al. (2012), this can have different reasons. One major point are the underlying choice of data sets (model runs, reanalysis, and/or observations). The definition of extreme events varies between certain thresholds, percentile-based indices, or return periods (e. g. Maraun et al., 2010). Other crucial points are that different time periods and areas were investigated as well as different model resolutions.

Spatially extended intensive rainfall events are frequently related to widespread flooding along the main river networks of central Europe causing major damage in the order of several billion euro (EUR) per event (e. g. Uhlemann et al., 2010; Kienzler et al., 2015; Schröter et al., 2015; MunichRe, 2017). Mudelsee et al. (2003) investigated the trends in the occurrence of extreme floods related to heavy precipitation events along the Oder and Elbe rivers. They found a decrease for winter floods in both river catchments, while there seems to be no significant trend for summer floods. In contrast, Dittus et al. (2016) found an increasing trend between 1951 and 2005 in extreme total precipitation amounts for e.g. Europe in global climate model simulations (CMIP5). Similar trends were found in reanalyses (e. g. ERA–20C, Poli et al., 2016), but not in observations. Moreover, Mudelsee et al. (2004) and Nissen et al. (2013) highlighted a strong dependency of central European flood events on the specific weather pattern of cyclone pathway “Vb” like the severe flood event of 2002 along the rivers Elbe and Danube (Ulbrich et al., 2003a, b). Such outstanding events are by definition extremely rare, which makes the risk estimation difficult or almost impossible due to the limited time period with available area-wide observations (e. g. Pauling and Paeth, 2007; Hirabayashi et al., 2013). Nevertheless, the estimation of flood risk and related trends for the past and the future are of great importance for insurance purposes or flood protection (e. g. Merz et al., 2014; Schröter et al., 2015; Ehmele and Kunz, 2019). A possible way of dealing with the unsatisfactory data availability are century-long simulations using climate models (e. g. Stucki et al., 2016) or stochastic approaches (e. g. Peleg et al., 2017; Singer et al., 2018; Ehmele and Kunz, 2019).

Several previous studies have investigated long-term trends and variability of extreme precipitation using century-long reanalysis data sets. For instance, Brönnimann et al. (2013) or Brönnimann (2017) analyzed historical extreme events and concluded that the quality of the reanalysis strongly depends on the number and type of the assimilated observations, mainly sea

https://doi.org/10.5194/esd-2019-47
Preprint. Discussion started: 2 September 2019


Earth System Dynamics Discussions
Open Access
EGU

level pressure and monthly mean sea surface temperature. The investigated historical events were reproduced, but the magnitudes were underestimated. A possible reason is the decreasing number and quality of observations in the early century and therefore a lack of assimilation data. The suitability of reanalysis data to investigate extreme precipitation for England and Wales was investigated by Rhodes et al. (2015). While time series of daily precipitation totals are well represented in both data sets, timing errors of heavy precipitation events were identified as one of the major problems. Stucki et al. (2012) investigated historical flooding events in Switzerland and indicate that the reanalyses underestimate precipitation in Switzerland which may result from the insufficient representation of the alpine topography. In addition, timing and the exact location of heavy precipitation were also found to be inaccurate.

In this study, a set of different realizations with one RCM is used and combined to the new ensemble LAERTES-EU (**LA**rge **E**nsemble of **R**egionla clima**T**e mod**E**l **S**imulations for **EU**rope). Basis is the global reanalysis data set 20CR (Compo et al., 2011), which was dynamically downscaled for Europe. Several studies highlighted the improvements of using high resolution RCMs for the investigation of climate extremes (e. g. Feser et al., 2011; Feldmann et al., 2008, 2013; Schewe et al., 2019), especially over complex terrain (e. g. Torma et al., 2015). LAERTES-EU consists of a handful of 20th century reanalysis data sets and a large ensemble of decadal hindcast simulations mainly for the second half of the century. Although all simulations were performed with the same RCM version and set-up, LAERTES-EU is a combination of different external forcings, boundary conditions, and/or assimilation. Projections for the upcoming decade will round up our analysis. The investigative focus lies on heavy precipitation in central Europe. LAERTES-EU is validated in terms of coincidence with observations, possible long-term trends and temporal variability.

The following research questions will be addressed.

(1) How well is extreme precipitation represented in the RCM ensemble LAERTES-EU?

(2) What is the added value of LAERTES-EU compared to other available data sets?

(3) Which temporal evolution and variability of extreme precipitation over central Europe manifest during the past and what are the differences between the simulations and observations?

(4) Which tendency is expected for the upcoming decade?

A better interpretation of RCM data and a more profound understanding of extreme precipitation may have several applications such as risk assessments. However, potential mechanisms behind temporal variances and trends as well as spatial and seasonal differences are not part of this paper and will be discussed in continuative studies.

This paper is structured as follows: The data sets which were used in this study are introduced in Sect. 2. Section 3 sums up the methods used for the analysis and the validation. In Sect. 4 LAERTES-EU is validated with observations for a reference period. The investigation of temporal variabilities and trends is given in Sect. 5. Finally, Sect. 6 gives a summary and lists our main conclusions.

https://doi.org/10.5194/esd-2019-47
Preprint. Discussion started: 2 September 2019


Earth System Dynamics Discussions

## 2 Data sets

Two different types of data sets are applied in this study: gridded precipitation data based on observations and, partly century-long, climate model simulations (LAERTES-EU). The observational data sets are primarily available for the second half of the 20th century and serve as reference data for the validation of the ensemble. For validation we compare LAERTES-EU with the global reanalysis data set of 20CR (Compo et al., 2011) as well, which were used as initial data for some of the RCM simulations.

### 2.1 Observations

The main reference for this study is the European observational data set E–OBS version v17 for daily precipitation (Haylock et al., 2008; van den Besselaar et al., 2011) with a horizontal resolution of 0.22° (≈ 25 km), covering the years 1950 to 2017. This version shows some improvements towards older versions, since updated algorithms and new stations have been included in some areas (e. g. for Poland). The E–OBS algorithm interpolates observations from weather stations to a regular grid using geostatistical methods (e. g. Journel and Huijbregts, 1978; Goovaerts, 2000). Note that E–OBS is a land-only data set, and ocean grid points are set to a missing value. Haylock et al. (2008) stated that rainfall totals in E–OBS are reduced by up to almost one third compared to the raw station data. Regarding extremes, the deviation of E–OBS is even more pronounced (Hofstra et al., 2009).

Additionally, we compare the RCM simulations with the high-resolved HYRAS data set provided by the German Weather Service (DWD; Rauthe et al., 2013). HYRAS is a gridded precipitation data set with a horizontal resolution of up to 1 km for the time period 1951–2006 and covers Germany and the surrounding river catchments. The HYRAS algorithm also uses ground based measurements and interpolates the point observations to the regular grid.

### 2.2 Regional climate model simulations

LAERTES-EU consists of a combined large downscaling ensemble of simulations with one RCM. There are two different types: long-lasting simulations of 45–110 years and simulations over one decade. In the latter, only a period of 10 years (e. g. 1961–1970) was simulated with a specific number of ensemble members. Then, the initialization point was shifted by one year (e. g. 1962–1971) and so on until the end of the covered time period. In total, LAERTES-EU consists of 1183 more or less independent simulations (sample size) with approximately 12.500 simulated years. The number of ensemble members at a specific time varies from 6 at the beginning of the century to a maximum of 188 members between 1970 and 2000 (see Fig. S1 in Supplementary).

LAERTES-EU is divided into four different data blocks (Table 1). All regional simulations used the non-hydrostatic model of the Consortium for Small-scale Modeling (COSMO) in climate mode model version 5 (CCLM5; Rockel et al., 2008) and have a spatial resolution of 0.22° (≈ 25 km). The model covers the EURO–CORDEX[1] domain (Jacob et al., 2014). All the

[1] http://www.euro-cordex.net

https://doi.org/10.5194/esd-2019-47
Preprint. Discussion started: 2 September 2019


Earth System Dynamics Discussions
Open Access
EGU

**Table 1.** Overview of the RCM ensemble LAERTES-EU with the name of the simulation, the classification into data blocks, the underlaying set-up (experiment), the covered time period, and the number of simulation years. For data blocks 2 and 4, period means the range of the initialization years; XX stand for the ensemble number and YYYY for the initialization year.

| name | block | experiment | period | years | comment |
|---|---|---|---|---|---|
| as20ncep**XX** | 1 | 20CR via MPI–ESM–LR | 1900–2009 | 330 | 3 members of 110 years each |
| dec**XX**o**YYYY** | 2 | MPI–ESM–LR DROUGHTCLIP | 1910–2009 | 3000 | 3 members with 100 decades each |
| historical_r**X**i1p1-HR | 3 | MPI-ESM–HR HISTORICAL | 1900–2005 | 410 | run 1–3 each with 106 years, |
| | | | | | run 4–5 each with 46 years (1960–2005) |
| preop | 4 | MPI–ESM–HR CMIP5 | 1960–2016 | 2850 | 5 members with 57 decades each |
| dcppA-hindcast | 4 | MPI–ESM–HR CMIP6 | 1960–2018 | 5900 | 10 members with 59 decades each |

simulations were performed within the BMBF (Federal Ministry of Education and Research of Germany) project MiKlip II[2] (Marotzke et al., 2016). For all simulations the same domain, model version and set-up, adapted from EURO–CORDEX, were used.

The boundary forcing was derived from the Max–Planck Institute of Meteorology coupled Earth System Model (MPI–ESM). This model consists of the atmospheric component ECHAM6 (Stevens et al., 2013), the ocean component MPI–OM (Jungclaus et al., 2013), and the land-surface model JSBACH (Hagemann et al., 2013). The differences between the four different data blocks stems from the setup, external forcing and initialization of the MPI–ESM simulations. The data blocks 1 and 2 of the RCM ensemble (cf. Table 1) obtained it boundary values from the MPI–ESM–LR simulations using a T63 resolution and 47 vertical layers. Data block 3 and 4 used the MPI–ESM–HR version (Müller et al., 2018) as their driving model. In this version, the horizontal resolution is T127 and 95 vertical layers are applied.

The MPI–ESM forcing data used for the three long-term simulations in data block 1 assimilated the 20th Century Reanalysis (20CR; Compo et al., 2011; Mueller et al., 2014) over the period 1900–2009. 20CR has a spatial resolution of approximately 2° (T62) and was generated using the Global Forecast System (GFS; Kanamitsu et al., 1991; Moorthi et al., 2001) of the National Centers for Environmental Prediction (NCEP)[3]. It used a 56 member Ensemble Kalman Filter approach to assimilate surface pressure, monthly sea surface temperature and sea-ice observations. From these simulations the starting conditions for a decadal hindcast ensemble (data block 2) has been derived (Mieruch et al., 2014; Mueller et al., 2014; Reyers et al., 2019; Feldmann et al., 2019). Each year three initialized decadal simulations were started, to study the long-term predictive skill on decadal time scales.

Data block 3 contains the downscaling of five un-initialized (historical) simulations of MPI–ESM–HR with CMIP5 observed natural and anthropogenic external forcing (Taylor et al., 2012). Data block 4 encompasses two sets of decadal hindcasts over

[2]https://www.fona-miklip.de/
[3]http://www.ncep.noaa.gov/

https://doi.org/10.5194/esd-2019-47
Preprint. Discussion started: 2 September 2019


Earth System Dynamics Discussions

the period since 1960 (Müller et al., 2012; Marotzke et al., 2016). The preop–ensemble has five members each year. The climate forcing for these simulations stems also from CMIP5, whereas for the 10 member per year dcppA–ensemble the CMIP6 external forcing was applied (Eyring et al., 2016; Boer et al., 2016).

The simulation in all four data blocks are affected by the observed climate forcing, but differ with respect to the representation of the observed climate variability, whereas data block 1 uses assimilated 20CR reanalysis data, block 2 and 4 contain initialized hindcasts and block 3 only uses the external forcing information. Nonetheless, the four groups of downscaling simulations can be grouped into a large ensemble, since the regional simulations were all performed with the same setup. The validity of this combination approach is tested within Sect. 4.

In order to reduce well-known limitations of climate model simulation, the ensemble data first were filtered using a dry–day adjustment. According to Feldmann et al. (2008), a dry–day correction is essential as climate models tend to overestimate the number of wet days with low intensities below 0.1 mm (Berg et al., 2012), known as the drizzle effect. The dry–day correction was performed using the E–OBS data, as it has the same spatial extension and resolution.

## 3 Methods

The capability of LAERTES-EU to simulate realistic precipitation amounts and distribution is an important requirement. Moreover, temporal variability and possible trends should also be well represented for trustworthy data sets. The methods were applied to different investigation areas and time periods. Equations and additional information can be found in Appendix A–C. As the focus of this study is heavy precipitation, we concentrate on high percentiles of spatially aggregated daily rainfall totals, namely 99 %, and 99.9 %.

### 3.1 Validation methods

LAERTES-EU is analyzed and validated using various methods. The intensity spectrum gives the statistical probability of each precipitation amount by taking into account all grid points and all time steps within the investigation area. Therefore, the range of occurred values is divided into evenly spaced histogram classes, which then are normalized with the total sample size. The resulting intensity–probability–curve (IPC) is a good indicator, if the model is capable to simulate realistic precipitation intensity distributions.

The quantile–quantile (Q–Q) plot compares the simulated distribution with the observed one using different percentiles of daily spatial mean precipitation. The Q–Q distributions are used to calculate the coefficient of determination $R^2$ with $R$ being the Pearson correlation coefficient (Eq. A1 in Appendix A).

The added value of the ensemble size is analyzed by using the signal–to–noise ratio $S2N$ (Eq. A4). Therefore, we determine a Gumbel distribution (cf. Appendix A) for different sample sizes and the corresponding 90 % confidence interval. The $S2N$, then, is the ratio of the return value of the Gumbel distribution divided by the 90 % confidence interval (Früh et al., 2010).

https://doi.org/10.5194/esd-2019-47
Preprint. Discussion started: 2 September 2019


Earth System Dynamics Discussions

### 3.2 Decadal variability and trend analysis

For the analysis of the temporal evolution of heavy precipitation we use time series of different percentiles of spatial mean precipitation and quantities introduced and recommended by the Expert Team on Climate Change Detection and Indices (ETCCDI; Karl et al., 1999; Peterson, 2005). Currently, 27 indices for temperature and precipitation are defined by the ETCCDI. These indices can be used from local to global scales. Additionally, they combine extremes with a mean climatological state (Zwiers et al., 2013). In this study, we use the two indices R95pTOT and R99pTOT (Eq. B1–B2 in Appendix B), which indicate the amount of precipitation above the 95 % or 99 % percentile, respectively.

In terms of trend analysis, a Mann–Kendall test (Mann, 1945; Kendall, 1955) is performed with related significance investigations (Appendix C). Regarding possible oscillations, the complete time series is split into sub-series with a minimum length of 10 years and up to 130 years (trend matrix). The Mann–Kendall test is applied to each of this sub-series.

### 3.3 Investigation areas and time periods

The focus of this study is central Europe, implying the countries Germany, Switzerland, the Netherlands, Belgium, Luxembourg, and parts of France, Poland, Austria, the Czech Republic, and Italy. Following Christensen and Christensen (2007), these countries are mostly coincident with two of the areas defined in the PRUDENCE project (prediction of regional scenarios and uncertainties for defining European climate change risks and effects), namely the PRUDENCE regions (PR) Mid–Europe (ME) and Alps (AL; Fig. 1).

The data sets are investigated on different time periods (TP): TP1 covers the past from 1900 to 2017, which is divided into a sub-period TP1b containing only the period with available observations from 1950 to 2017 (E–OBS). The time period TP2 is used for the predictions from 2018 to 2028. For climatological aspects, we use the time period 1961–1990, hereafter referred to as climTP.

## 4 Validation of the RCM ensemble

In the following, the above described methods are applied in order to validate LAERTES-EU concerning its representativeness with observations. With this aim, data for the investigation period TP1b is used.

### 4.1 Statistics

The IPCs give the range of simulated (observed) precipitation intensities at any grid point in the investigation area and its corresponding probability (Fig. 2). For both investigation areas, the IPCs reveal a distinct added value of the RCM compared to the global model. Due to the coarse resolution, the GCM is incapable of simulating intensities greater than approximately $60\,\mathrm{mm\,d^{-1}}$ and underestimates by a large degree the probability of a wide range of intensities. On the other hand, the RCM tend to overestimate precipitation intensities and the IPCs lie above those of the observations but cover the entire range of values. For Mid–Europe (Fig. 2a), the IPCs of the RCM are close to HYRAS, but there is a systematic difference between

https://doi.org/10.5194/esd-2019-47
Preprint. Discussion started: 2 September 2019


Earth System Dynamics
Discussions
Open Access
EGU

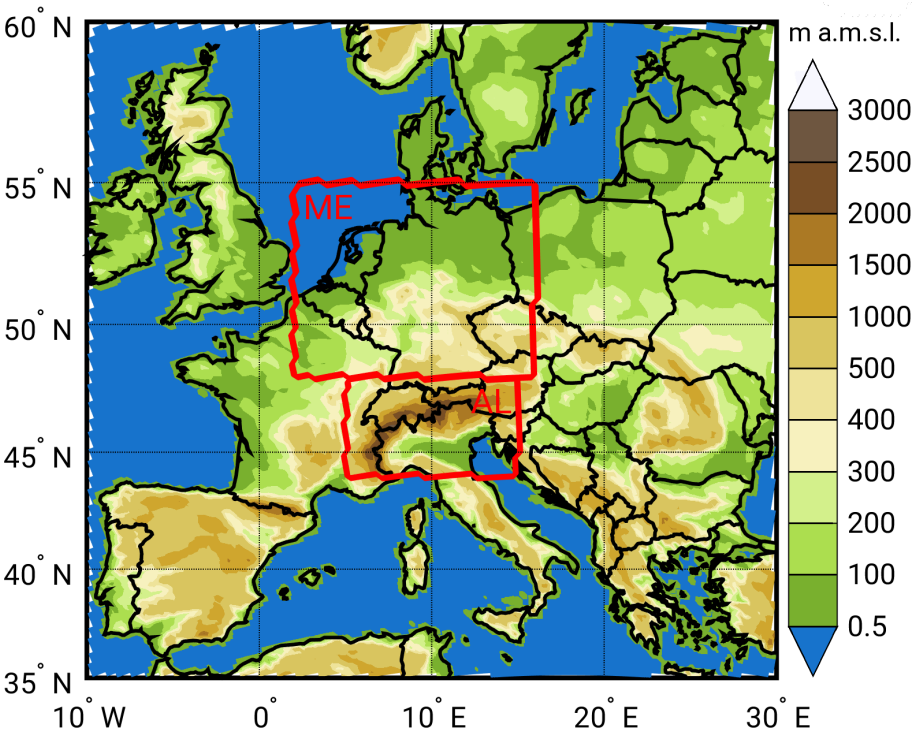


**Figure 1.** Topographic map of Europe at model resolution 0.22° with the PRUDENCE regions ME and AL (red boxes) and state borders (black contours).

HYRAS and E–OBS. As already mentioned by Haylock et al. (2008), E–OBS has a certain negative bias up to –30 %. The given deviation between HYRAS and E–OBS is in between this range. For the Alpine region (Fig. 2b), the IPCs of E–OBS and HYRAS are almost identical with values up to 200 mm $d^{-1}$. The difference between the RCM simulations and the observations at a given probability again is in order of 20 %, thus within the E–OBS uncertainty. For both investigation areas the range of simulated values is much higher with up to 470 mm $d^{-1}$. Note that only a small part of AL is covered by HYRAS which might be a reason for the vanished differences between E–OBS and HYRAS and the resulting specious deviations to the RCM.

A direct linkage between observed and simulated precipitation is given by a Q–Q plot (Fig. 3). Therefore, daily spatial mean precipitation fields for both investigation areas are used. Then, the distributions for these values are calculated. Generally speaking, the distribution of the RCM is in better agreement with the observations, at least with E–OBS, with little deviations from the optimum (diagonal line) for most of the spectrum and differences at around 10 % for the upper part of the distribution. In comparison to HYRAS, the maximum deviation is higher with around 20 %. For AL (Fig. S2), the RCM data differs more and over a wider range of the spectrum compared to HYRAS than for ME. Even though HYRAS was aggregated to the E–OBS / RCM grid, the more pronounced differences especially for the extremes might be a result of the higher resolution of the HYRAS data, which, in particular, is of greater relevance in the mountainous region of AL.

https://doi.org/10.5194/esd-2019-47
Preprint. Discussion started: 2 September 2019


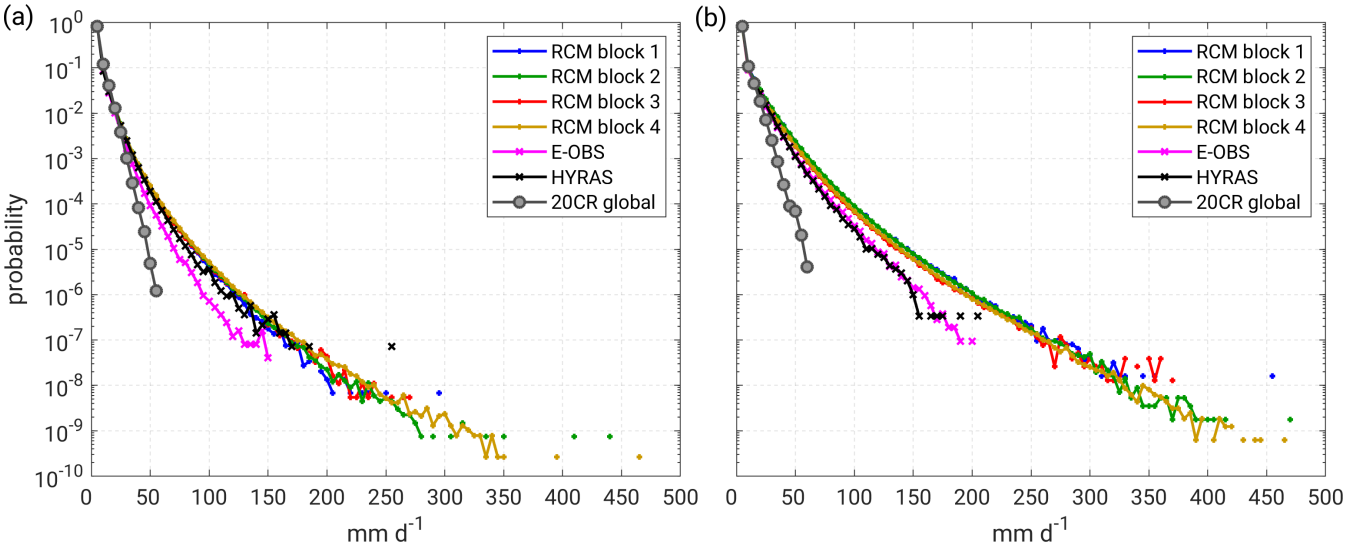


**Figure 2.** Intensity–probability–curve (IPC) of daily rainfall totals of the RCM simulations (dry–day adjusted), observations (E–OBS and HYRAS) and global reanalysis (20CR) for (a) Mid–Europe (ME) and (b) the Alps (AL) during the investigation period TP1b.

**Table 2.** Coefficients of determination $R^2$ between the RCM and observations for the quantile–quantile contemplation of Fig. 3 for Mid–Europe (ME) and the Alps (AL).

| RCM | E–OBS | | HYRAS | |
|---|---|---|---|---|
| | ME | AL | ME | AL |
| Data block 1 | 0.9914 | 0.9924 | 0.9876 | 0.9835 |
| Data block 2 | 0.9914 | 0.9925 | 0.9878 | 0.9848 |
| Data block 3 | 0.9963 | 0.9976 | 0.9936 | 0.9930 |
| Data block 4 | 0.9966 | 0.9981 | 0.9943 | 0.9938 |

215 The findings of Fig. 3 are confirmed by the determination coefficients $R^2$ (Table 2). For both E–OBS and HYRAS the coefficient is very high with $R^2 > 0.98$. There is a slightly higher $R^2$ for E–OBS than for HYRAS, which is an artificial effect of the data resolution. The region AL shows a minimal higher skill compared to ME in E–OBS and slightly lower values in HYRAS. Table 2 also reveals higher correlations of the CCLM simulations driven by the high resolution MPI–ESM–HR compared to those driven by the lower resolved MPI–ESM–LR data.

https://doi.org/10.5194/esd-2019-47
Preprint. Discussion started: 2 September 2019


Earth System Dynamics
Discussions
Open Access
EGU

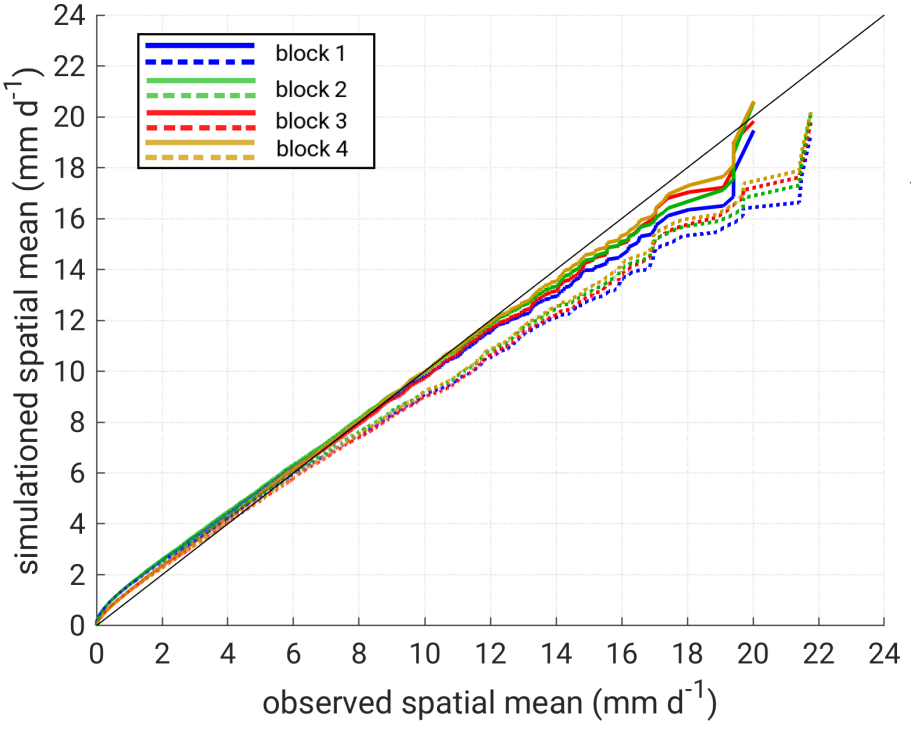


**Figure 3.** Quantile–quantile plot of spatial mean daily precipitation for investigation period TP1b comparing the RCM simulations (data block 1–4) with E–OBS (solid lines) and HYRAS (dashed lines) for Mid–Europe (ME).

### 4.2 Time series

Beside overall statistics, other properties of LAERTES-EU like the temporal variability should cover the range of observations as well. Therefore, we analyze the time series of yearly values of different percentiles of the spatial mean precipitation for the investigation areas. In Fig. 4 the time series of the 99 % percentile for ME is shown. Both observational data sets have a high year–to–year variability with similar shape but the mean over TP1b is about 10 % higher in HYRAS than in E–OBS. The ensemble mean value is very close to the E-OBS mean with relative deviations between –5 % and 4 %, and 0.6 % on average during TP1b. Compared to HYRAS the differences are –14 to –5 % with –8 % on average. The spread of both observational data sets is covered by the ensemble spread except for few extreme peaks (e. g. 1985 in E–OBS or 1998 in HYRAS). In AL, the HYRAS mean is about 15 % higher than E–OBS but both time series have again a similar shape (Fig. S3). The ensemble mean in this area lies within both observation means and a little closer to HYRAS. The relative deviation is 6–15 % (10 % on average) to E–OBS and –8 to 0.2 % (–5 % on average) to HYRAS. The ensemble spread also covers the observed variability.

Regarding more extreme values, namely the 99.9 % percentile, similar results can be found. E–OBS shows a certain bias to HYRAS of approx. 10 % for ME and 25 % for AL (Fig. S4 and S5). The ensemble mean is close to E–OBS with a deviations of –10 to 1 % (–3 % on average) for ME, and 6 to 16 % (10 % on average) for AL. Compared to HYRAS, LAERTES-EU differs

https://doi.org/10.5194/esd-2019-47
Preprint. Discussion started: 2 September 2019


Earth System Dynamics Discussions
Open Access
EGU

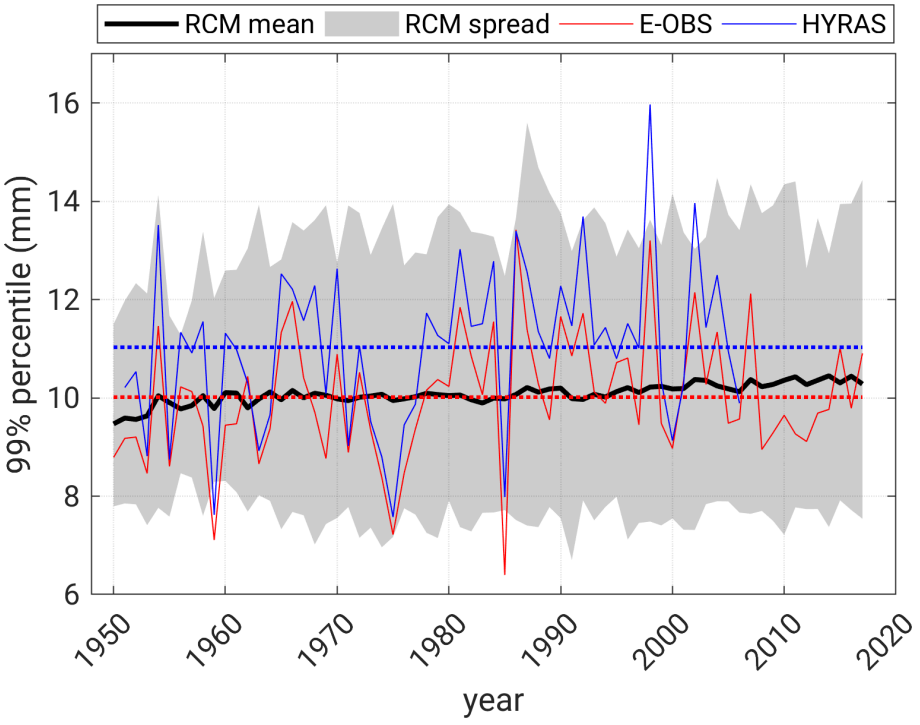


**Figure 4.** Time series of the yearly 99 % percentile of spatial mean precipitation for Mid–Europe (ME) during TP1b of the LAERTES-EU ensemble mean (black), the ensemble spread (minimum to maximum; gray), E–OBS (red), and HYRAS (blue). The dotted lines symbolize the mean values of the observations throughout TP1b.

between –19 and –7 % (–11 % on average) in ME, and between –18 and –10 % (–15 % on average) in AL. Furthermore, there is a distinctly higher spread and variability of the 99.9 % for both, the observations and LAERTES-EU. Again, the minimum values of the ensemble spread seem to be constant over time, while there is an increase in the maximum values for ME but no clear signal for AL. Except for a few peaks, LAERTES-EU covers the spread of the observations.

### 4.3 Added value of the sample size

In order to demonstrate the added value of the presented LAERTES-EU we use the signal–to–noise ratio ($S2N$, Eq. A4) for different sample sizes and return periods (cf. Appendix A). Sample size, in this case, means the number of data which is equivalent with the number of simulation runs. Observations have a sample size of 1. For both ME and AL, the $S2N$ increases with the sample size meaning a more statistically robust estimate of the return values (Fig. 5). At the beginning there is a strong increase of $S2N$ until a sample size of approximately 10. Between a sample size of 10 to 100 the increase of $S2N$ is weak. This range is typically used as ensemble size. For a sample size of 100 and more $S2N$ increases rapidly.

Furthermore, the $S2N$ is lower for higher return periods which is a result of less or even no data for very high return periods. However, $S2N$ also increases with sample size for the very high return periods. The robustness of a 2–year return

https://doi.org/10.5194/esd-2019-47
Preprint. Discussion started: 2 September 2019


Earth System Dynamics
Discussions
Open Access
EGU

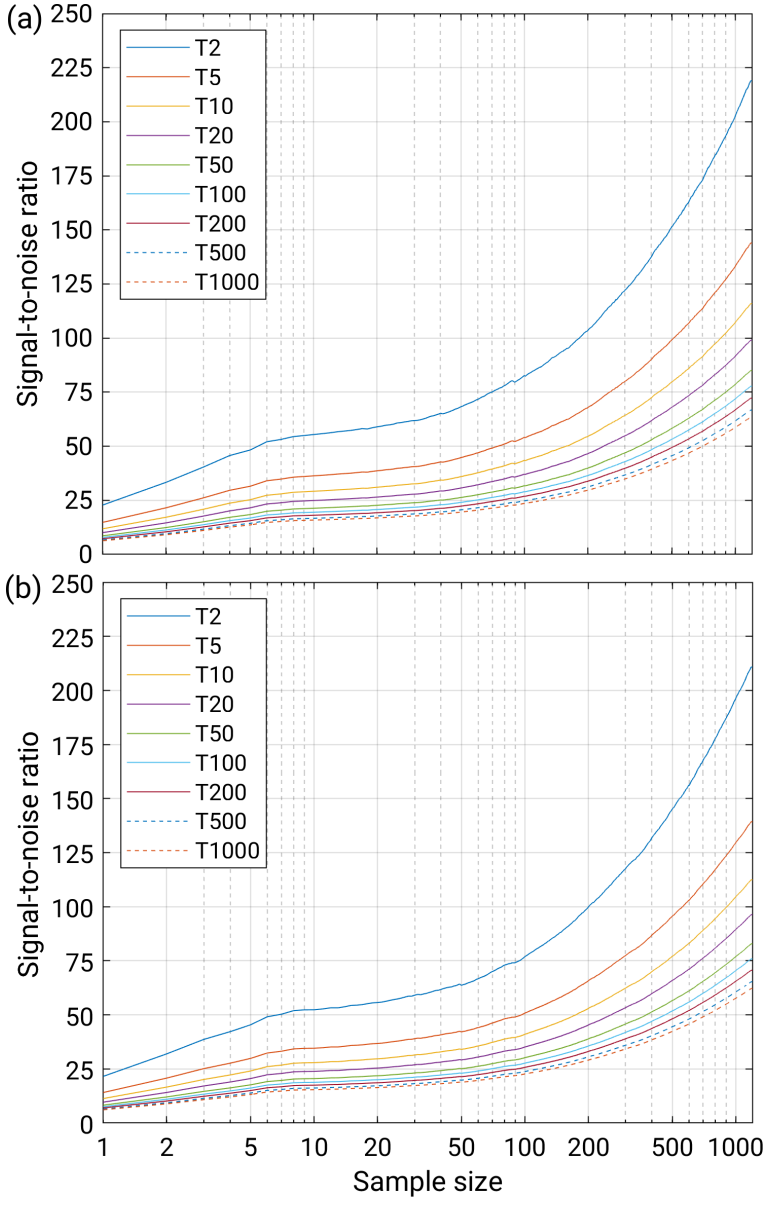


**Figure 5.** Signal–to–noise ratio for different return periods $T$ (colored lines) dependent on the sample size for (a) ME and (b) AL.

value estimate of a sample of size 20 is about the same as the 1000–year estimate for a sample of size 1000. This means that even for extremes, which have not been observed yet, some robust statistical analysis can be carried out.

https://doi.org/10.5194/esd-2019-47
Preprint. Discussion started: 2 September 2019


Earth System Dynamics
Discussions
Open Access
EGU

## 5 Long-term variability and trends

The temporal evolution and variability of extreme precipitation throughout the entire time period TP1 and also for predictions of the upcoming decade (TP2) is evaluated in this section. Beside time series of percentiles, we use climate change indices and statistical distributions.

### 5.1 Precipitation distributions

Figure 6 shows the evolution of the distribution of spatial mean precipitation throughout TP1 and TP2 by treating each decade independently. For the core of the distributions, namely medians, interquartile ranges, and upper whiskers, only small variances can be found between the different decades which means that there is almost no change for the majority of the precipitation amounts. Nevertheless, a marked positive trend for the uppermost extremes of the distributions appears with maximum values around 18 mm $d^{-1}$ at the beginning of the 20th century and about 24 mm $d^{-1}$ in the 21st century. The distribution for the upcoming decade 2020–2028 (Figure 6, green boxplot) shows only minimum differences to those of the present decade since 2010 with an almost equal median and interquartile range, but slightly higher maximum values.

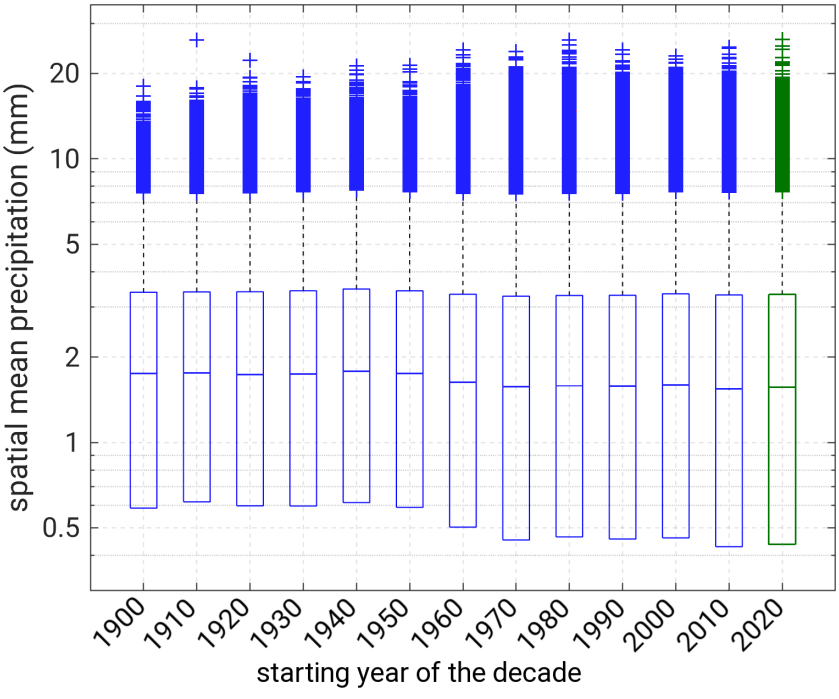


**Figure 6.** Boxplot of the distribution of daily spatial mean precipitation values for ME. Each decade during TP1 (blue) was considered separately. The centerline of a box marks the median; the lower and upper end of the box mark the 25th and 75th percentile (interquartile range); the whiskers represent approximately the 99.9 % percentile; TP2 is marked in green.

https://doi.org/10.5194/esd-2019-47
Preprint. Discussion started: 2 September 2019


Earth System Dynamics
Discussions
Open Access
EGU

The boxplot for AL is shown in Fig. S6 and illustrates that not only the high percentiles reveal a decrease in the middle of the century, but the entire distribution is shifted towards lower values. Nevertheless, there is no clear tendency for the maximum values. For TP2 (Fig. S6, green boxplot) the distribution is similar to that of the present decade in case of median and the upper part of the distribution. The interquartile range is reduced due to a increased lower boundary of the boxplot.

## 5.2 Temporal evolution of yearly percentiles

### 5.2.1 Overview

The overall trend during TP1 and TP2 using a linear regression for both areas and percentiles is given in Table 3. While the ensemble mean shows a significant positive trend for ME for both percentiles, a small but significant negative trend can be found for the 99 % of AL, while there is almost no change in the 99.9 % of AL. In all cases the ensemble spread increases due to both a decrease of the minimum values and an increase of the maximum values both being highly significant. The change of the maximums is stronger than the reduction of the minimums and more pronounced in AL than in ME.

**Table 3.** Overall trend during TP1 and TP2 using a linear regression of the yearly series of the 99 % and 99.9 % percentile (pct) for ME and AL; Given are absolute values and the relative changes (RC) compared to the climatological mean (climTP) for the minimum (min), the mean, and the maximum (max) percentile values, and the related significance (p–value).

| area | pct | variable | trend (mm) | RC (%) | climTP (mm) | $p_\alpha$ |
|---|---|---|---|---|---|---|
| ME | 99 | min | –0.4 | –5.3 | 7.5 | 0.9966 |
| | | mean | 0.7 | 7.0 | 10.0 | 1.0 |
| | | max | 2.6 | 19.0 | 13.7 | 1.0 |
| ME | 99.9 | min | –0.7 | –7.8 | 9.0 | 0.9974 |
| | | mean | 1.1 | 8.2 | 13.4 | 1.0 |
| | | max | 7.2 | 33.2 | 21.7 | 1.0 |
| AL | 99 | min | –2.6 | –17.8 | 14.6 | 1.0 |
| | | mean | –0.3 | –1.5 | 20.2 | 0.9381 |
| | | max | 4.4 | 15.9 | 27.7 | 1.0 |
| AL | 99.9 | min | –3.8 | –21.3 | 17.8 | 1.0 |
| | | mean | –0.0 | –0.0 | 27.3 | 0.0 |
| | | max | 8.3 | 18.9 | 44.0 | 1.0 |

https://doi.org/10.5194/esd-2019-47
Preprint. Discussion started: 2 September 2019


Earth System Dynamics
Discussions
Open Access
EGU

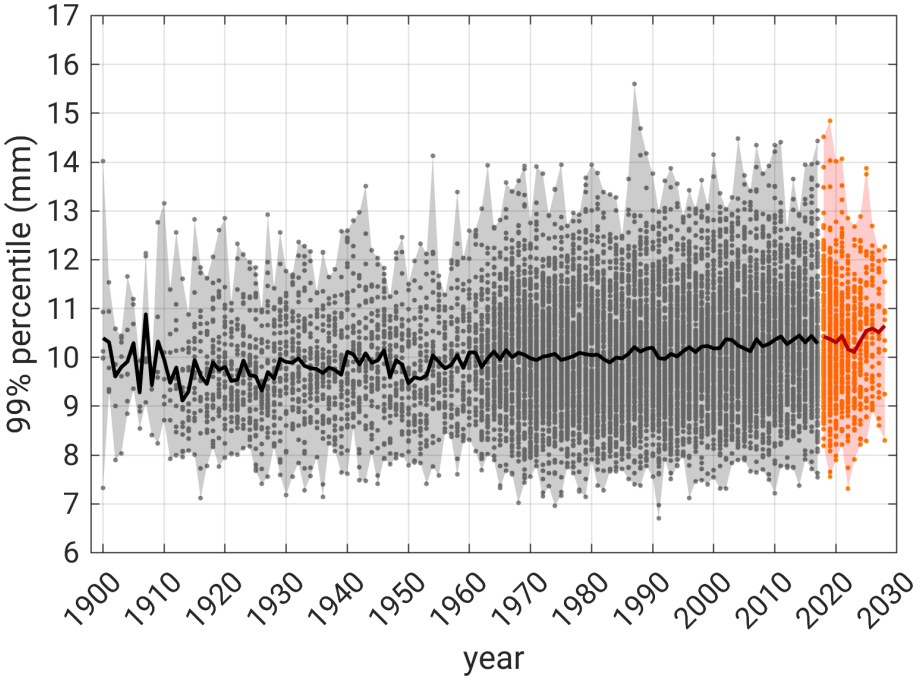


**Figure 7.** Time series of the yearly 99 % percentile of spatial mean precipitation for Mid–Europe (ME) of the LAERTES-EU ensemble mean (solid line), and the ensemble spread (dots and shaded area) during TP1 (black/gray) and TP2 (reddish).

Analogous to Table 3 we analyze the trend for TP1b only (Table S1 in Supplementary). The tendencies are the same for all cases but less pronounced except for the mean 99.9 % of AL where the negative trend during TP1b is slightly stronger than for the whole time series.

Figure 7 shows the temporal evolution of the 99 % percentile during the 20th and the beginning of the 21st century for the whole LAERTES-EU. As given in Table 3, the lower boundary changes are small, while there is a visible positive trend of the ensemble mean and the upper boundary of the ensemble spread. Note that the larger spread from the 1960s onwards might be artificial due to the decisively larger number of members of data block 4. Nevertheless, there is a clear consistency in the time series for ME.

Some differences emerge for the Alpine region AL (Fig. S7). At first, there is a distinct decrease of the ensemble mean between 1960 and 1970 which might reveal from the rising number of members. As the ensemble matches well with the observations, we presume an overestimation of precipitation in the first half of the 20th century in that region, which could be a result of missing data for the applied dry–day correction. Due to the more complex terrain, the structure of the precipitation fields is more complex, and therefore more sensitive for different types of effects such as the dry–day correction.

The results for the 99.9 % percentile are similar for both areas (Fig. S8 and S9). The positive trend for ME is even more pronounced, while the drop in the 1960s for AL is less visible and therefore the time series is more constant.

https://doi.org/10.5194/esd-2019-47
Preprint. Discussion started: 2 September 2019


Earth System Dynamics Discussions
Open Access
EGU

**Table 4.** Climatological mean 1961–1990 (climTP) of days per year exceeding the 99 % and 99.9 % percentile (pct) for ME and AL, linear regression (LR) and relative change (RC) compared to climTP for different investigation periods (TP), and related significance (p–value).

| area | pct | climTP | TP | LR | RC | $p_\alpha$ |
|---|---|---|---|---|---|---|
| ME | 99 | 3.77 | 1+2 | 1.39 | 37 % | 1.0 |
| | | | 1b | 1.11 | 29 % | 1.0 |
| | 99.9 | 0.62 | 1+2 | 0.36 | 57 % | 1.0 |
| | | | 1b | 0.27 | 43 % | 1.0 |
| AL | 99 | 3.81 | 1+2 | –0.26 | –7 % | 0.9618 |
| | | | 1b | –0.58 | –15 % | 0.9964 |
| | 99.9 | 0.62 | 1+2 | –0.01 | –2 % | 0.6825 |
| | | | 1b | –0.01 | –1 % | 0.3775 |

Taking a look into the evolution of the number of days exceeding the climatological mean percentile, a strong positive and significant trend appears for ME for both the 99 % (Fig. 8, top) and 99.9 % percentile (Fig. S10). The exact values of the climTP mean, the linear regression, the relative change, and the significance can be found in Table 4 (top numbers). For the Alpine region, the year–to–year variability is higher and the overall trend is slightly negative (Fig. 8, bottom, and S11) and at least significant for the 99 % percentile. Again, we analyze the trend for TP1b separately (Table 4, bottom numbers). the tendencies for TP1b are the same but less pronounced except for the days exceeding the 99 % percentile in AL, where there is a stronger trend signal in TP1b compared to the whole time series, which is also significant to a high degree.

### 5.2.2 Past trends and oscillations

For a more detailed analysis of trends, the method described in Sect. 3.2 is applied to the time series of daily spatial mean precipitation. Figure 9a shows the number of LAERTES-EU members (relative) with a positive or negative trend of the 99 % percentile for ME. Only cases in which more than 60 % of the complete ensemble members reveal the same tendency are then considered for further investigations. For these cases the mean trend is calculated (Fig. 9b) and the relative amount of significant members is displayed (Fig. 9c). All cases in which the ensemble reveals ambiguous tendencies are neglected (gray areas).

To a high degree the single members show the same behavior, especially for the longer time series where positive trends are dominant. On a decadal time scale (diagonal line in Fig. 9) some oscillations appear with phases of increasing and decreasing precipitation. This signal might be smoothed as it is not expected that the decadal simulations of data blocks 2 and 4 cover the natural variability at this time scale in detail. Furthermore, these simulations are not expected to be in phase with the long lasting simulations of data blocks 1 and 3. The trends on this time scale reach rates of up to 0.1 mm $a^{-1}$ or 1 mm per decade,

https://doi.org/10.5194/esd-2019-47
Preprint. Discussion started: 2 September 2019


Earth System Dynamics
Discussions
Open Access
EGU

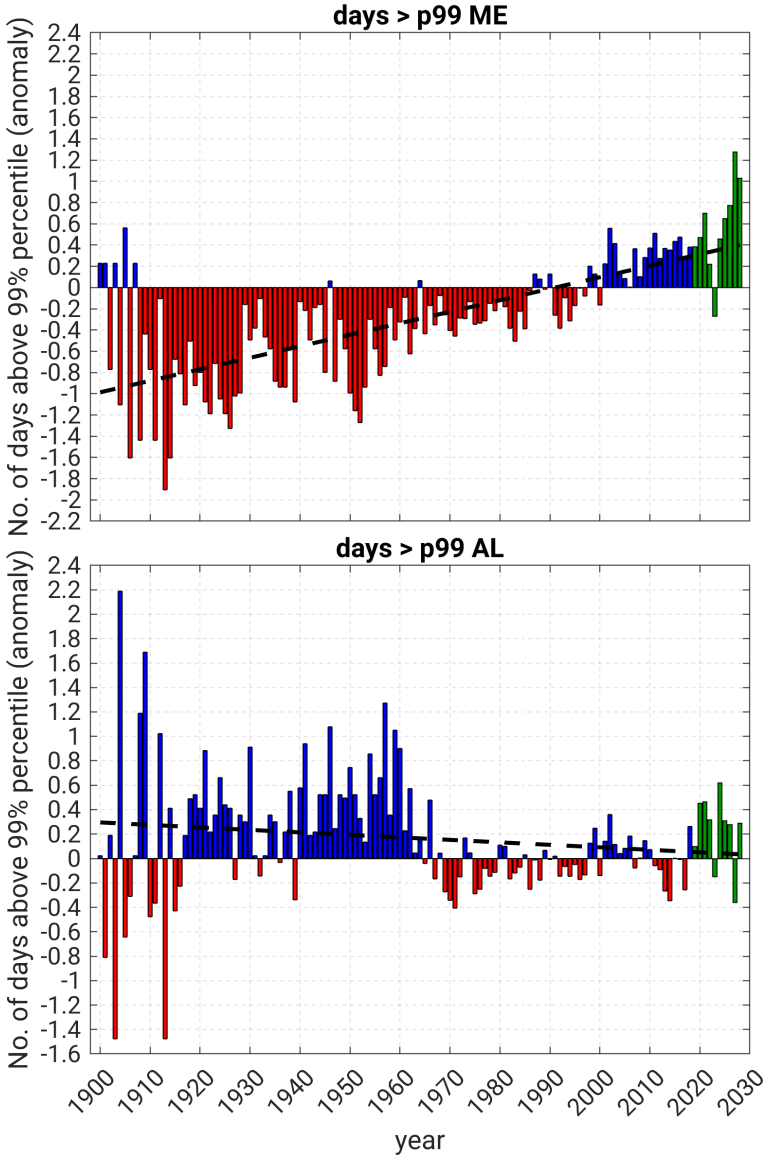


**Figure 8.** Deviation of the mean yearly number of days above the 99 % percentile compared to the climatology (1961–1990; climTP) for ME (top) and AL (bottom). Red bars indicate negative anomalies (less days), blue bars positive anomalies (more days). The predictions (TP2) are given in green. The black line indicates a linear regression.

respectively. The overall trend is weaker with rate of 0–0.02 mm $a^{-1}$ or 0–2 mm per century, respectively. Positive trends are more often significant than the negative, while only a small part of the ensemble shows significant trends. Similar results can be found for the Alpine region (Fig. S12). The trends on the decadal time scale reach higher rates but the oscillation is less

https://doi.org/10.5194/esd-2019-47
Preprint. Discussion started: 2 September 2019


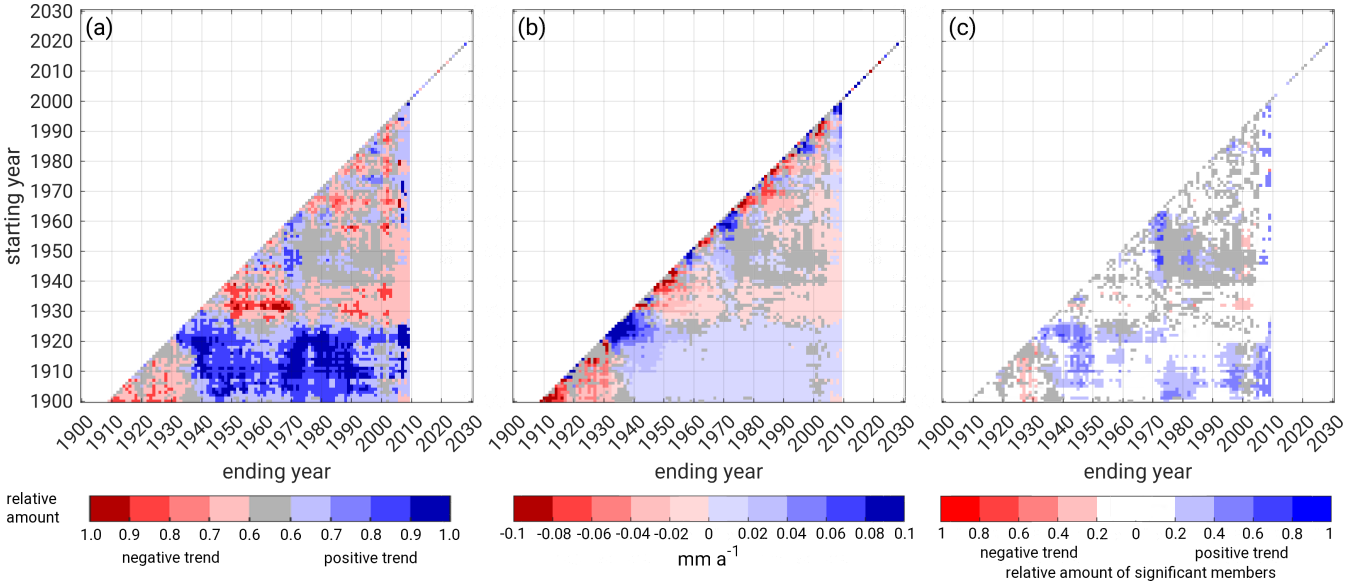


**Figure 9.** Trend analysis of the 99 % percentile for ME with (a) the relative amount of members of LAERTES-EU with a positive (blue) or negative (red) trend; (b) the trend in mm per year averaged over the members from (a), and (c) relative amount of members from (a) that have a significant trend; cases with no distinct number (less than 60 %) of members with same trend sign are marked in gray in (a)–(c).

pronounced than in ME. Again, most of the positive trends are significant, while just a few members with negative trends are significant.

For the 99.9 % percentile of ME (Fig. S13) large parts of LAERTES-EU show positive trends. On the decadal time scale a clear sequence of positive and negative trends is visible. Both the increases and decreases are more pronounced than for the 99 % percentile but only a few members are significant. In the Alpine region (Fig. S14) even more parts of the ensemble have the same tendency of heavy precipitation and a higher number of members have a significant trend. These trends exceed rates of decisively more than $\pm 0.1$ mm a$^{-1}$. In contrast to the results above, the 99.9 % percentile for AL seems to have a multidecadal oscillation, while the overall trend of the complete time series is negative.

### 5.2.3 Future projections

With respect for the upcoming decade (TP2), LAERTES-EU predicts an continuation of the current trend with an increase especially for the 99.9 % percentile (Fig. 7, and S6–S8; reddish area). In comparison to the last decade (2007–2017), the RCM mean of the 99 % percentile increases of about 0.6 % for ME and about 2.1 % for AL. The 99.9 % percentile increases about 2.0 % for ME and 3.0 % for AL. Further to this absolute change, the number of days exceeding the climatological 99 % percentile shows an increase of 4.9 % for ME and 8.4 % for AL, and 6.7 % (ME) and 22.4 % (AL) in case of the 99.9 % compared to the mean of 2007–2017. This also manifests in the relative anomaly (Fig. 8, and S9–S10; green bars).

https://doi.org/10.5194/esd-2019-47
Preprint. Discussion started: 2 September 2019


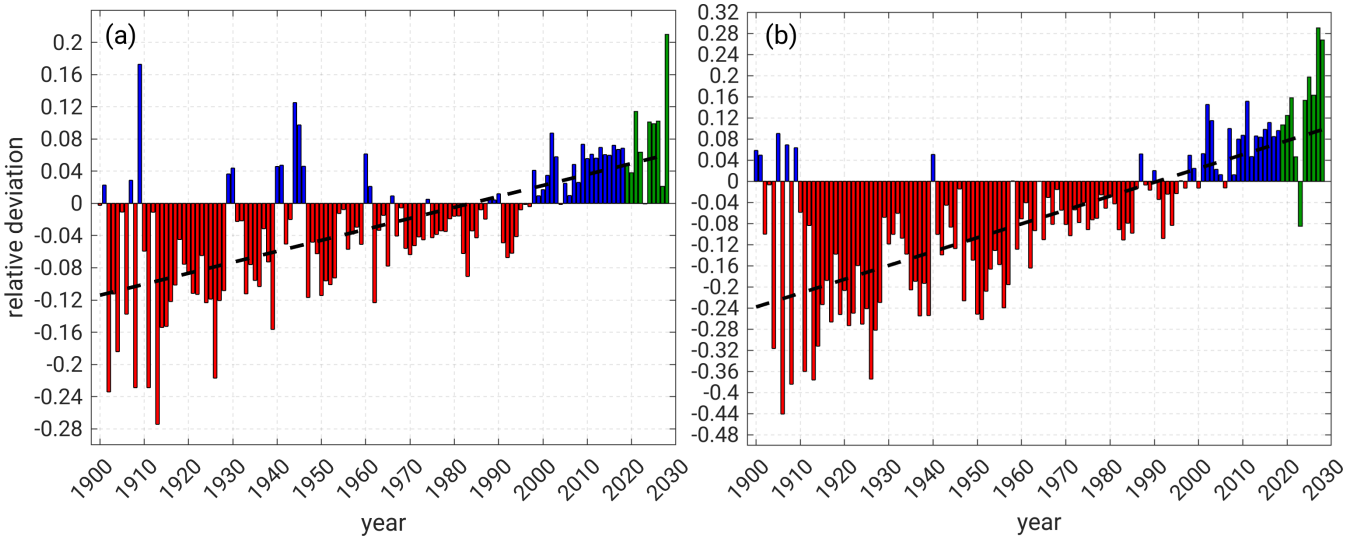


**Figure 10.** Relative deviation of (a) the R95pTOT index and (b) the R99pTOT index of the LAERTES-EU mean compared to the climatology (climTP) for ME. Red bars indicate negative (dry) anomalies, blue bars positive (wet) anomalies. The predictions (TP2) are given in green. The black line indicates a linear regression.

Nevertheless, a more detailed trend analysis illustrated in Fig. 9 and also Fig. S12–14 reveals that LAERTES-EU shows no clear tendency for the 99 % for TP2. Just in a few cases more than 60 % of the members have a similar mainly positive trend signal, which however is not significant. In case of the 99.9 % percentile, 60–70 % of the members show a strong positive trend of more than 0.1 mm $a^{-1}$ with 20–40 % of them being significant. Although the tendency for TP2 is ambiguous and less significant, it shows continuity to the present decade and so we conclude that a positive trend is likely.

### 5.3 Climate change indices

The results described in the previous section also manifest in the considered ETCCDI climate change indices (Table 5). R95pTOT shows a positive trend for ME (Fig. 10a) with a relative change of about 17 % and a strong negative trend of approximately –15 % for AL (Fig. S15). Remarkably, there is a high positive deviation in the early 20th century compared to the climTP amount for AL which might be artificial due to the mentioned problems of the dry–day correction. R99pTOT shows a positive change for ME (Fig. 10b) and slightly negative trend for AL (Fig. S16). The overemphasis for AL in the early century is less pronounced for this index. Considering only the TP1b, the tendencies are the same in all cases. The positive trends for ME are less pronounced, while the negative trends for AL are stronger. The estimated trends are highly significant except for the R99pTOT of AL for the whole time series.

Compared to the present decade, the projections show a continuation of the positive trend for ME with an increase of 2 % for R95pTOT and 5 % for R99pTOT. In contrast, both indices show a positive trend for AL with an increase of 7 % for R95pTOT and 8 % for R99pTOT, which is a complete reversion of the overall trend.

https://doi.org/10.5194/esd-2019-47
Preprint. Discussion started: 2 September 2019


Earth System Dynamics Discussions

**Table 5.** Climatological mean 1961–1990 (climTP) of ETCCDI quantities for ME and AL, linear regression (LR) and relative change (RC) compared to climTP for different investigation periods (TP), and related significance (p–value).

| area | ETCCDI | climTP (mm) | TP | LR (mm) | RC (%) | $p_\alpha$ |
|---|---|---|---|---|---|---|
| ME | R95pTOT | 162.7 | 1+2 | 28.4 | 17 | 1.0 |
| | | | 1b | 20.1 | 12 | 1.0 |
| | R99pTOT | 46.3 | 1+2 | 15.6 | 34 | 1.0 |
| | | | 1b | 12.2 | 26 | 1.0 |
| AL | R95pTOT | 304.9 | 1+2 | –46.3 | –15 | 1.0 |
| | | | 1b | –54.3 | –18 | 1.0 |
| | R99pTOT | 88.9 | 1+2 | –4.5 | –5 | 0.8953 |
| | | | 1b | –10.8 | –12 | 0.9891 |

## 6 Summary and Conclusions

We have presented a novel combined ensemble LAERTES-EU of various regional climate model simulations to better estimated heavy precipitation across central Europe. The whole RCM ensemble was divided into four data blocks depending on forcing data, assimilation schemes, or the initialization of the driving global MPI–ESM. In total, the presented LAERTES-EU consists of over 1100 simulation runs with approximately 12.500 simulated years on a 25 km horizontal resolution.

The focus of investigation was laid on the PRUDENCE regions Mid–Europe (ME) and Alps (AL). Regarding heavy precipitation we concentrated on high percentiles, namely 99 % and 99.9 %. It was not expectable that the simulations are able to reproduce precipitation events on a daily base in detail, but have a better performance regarding long-term variations, and statistical distributions. Furthermore, the given resolution restricts the consideration of convective processes, so we analyzed time series of spatial mean precipitation.

With respect to our research questions, the following main conclusions can be drawn out of the presented results:

(1) Extreme precipitation is well represented in LAERTES-EU. The four data blocks are consistent and have similar precipitation distributions (IPCs), which are within the uncertainty of the observations. The ensemble range covers the observed temporal evolution.

(2) The added-value of the large ensemble size manifests in a strong increase of the signal–to–noise ratio beyond the typically used ensemble sizes and in high statistical significances of estimated trends for the ensemble mean.

https://doi.org/10.5194/esd-2019-47
Preprint. Discussion started: 2 September 2019


Earth System Dynamics Discussions

(3) Long-term trends reveal spatial differences in sign and strength and between the members. These tendencies are partly significant. Distinct oscillations can be found on shorter time scales (e. g. decades).

(4) The projections for the upcoming decade show a continuation of past tendencies with increasing heavy precipitation without any discontinuity. However, LAERTES-EU shows no clear signal and less significance for the projections.

Regarding the validation (1), intensity–probability–curves (IPCs) and Q–Q distributions have been analyzed. In all cases the IPCs of the simulations show an overestimation of precipitation compared to E–OBS of about one third. Haylock et al. (2008) found out that E–OBS has a certain negative bias of up to 30 % compared to raw observations. Taking this into account the IPCs are almost coincident. Nevertheless, the IPCs of LAERTES-EU show only small deviation compared to the high resolution HYRAS data set. Distinct differences mainly appear in the Alpine Mountains, which can be explained by less spatial coverage of observations. Furthermore, the IPCs and Q–Q distributions of all four data blocks are coincident which was a prerequisite for the combination to one large ensemble. The Q–Q distributions reveal less differences between modeled and observed precipitation compared to E–OBS and an underestimation of simulated rainfall compared to HYRAS by about 10 %.

Regarding (2), LAERTES-EU reveals a clear added value due to the large sample size. Estimates of long return periods are more robust compared to smaller ensembles. Furthermore, trends at least in the ensemble mean are highly significant. The IPCs also show a clear added value of RCM data compared to coarser global models. Regarding extremes, LAERTES-EU includes a broader range of precipitation totals which are not covered by observations due to their limited temporal availability.

Besides a proper representation of precipitation, long-term trends and temporal variations were of special interest. Regarding (3), the presented results show a good agreement of LAERTES-EU concerning the temporal evolution of the considered percentiles of spatially aggregated daily precipitation totals for the different investigation areas. The ensemble mean is within the range of the observations and the spread (min–to–max) covers the observed variability except a few peaks. Throughout the complete TP1, positive and significant trends can be found for ME in both percentiles and also in the number of days exceeding the climatological mean (1961–1990). For AL, there is no clear trend signal in the ensemble mean but an increase in the maximum values. In contrast the number of days exceeding the climatology is decreasing. The positive trends for ME with relative changes about 7–8 % are coincident with the theoretical 6–7 % per Kelvin temperature change (CC rate) as Moberg et al. (2006) found an increase of approximately 1 K during the 20th century for Europe. The negative trends for AL, however, do not fit in this theoretical estimate. The maximum simulated percentile values increase with a super–CC rate up to a factor 4.

Comparing the trends of TP1 to the shorter TP1b, the tendencies are the same but less pronounced in TP1b. On a decadal time scale some oscillations can be found with periods of increasing precipitation and such with decreasing values. Similar results as for time series of percentiles can be found using climate change indices (ETCCDI).

Regarding (4), the projections for the upcoming decade until 2028 (TP2) reveal ongoing tendencies of heavy precipitation indices. A special case is the Alpine region where the slightly negative trends in the past (TP1) turn to positive once. Both the continuity for ME and the reversion for AL appear in all time series, number of days or ETCCDI variables and all percentiles. While there is a clear signal and high significance building the ensemble mean first, the trends are ambiguous and less significant

https://doi.org/10.5194/esd-2019-47
Preprint. Discussion started: 2 September 2019




when considered separately. However, we conclude that this tendencies are likely as it is a continuation of the results of the present decade. Similar results for parts of LAERTES-EU were found by Reyers et al. (2019).

The presented LAERTES-EU data set can be used for various applications. However, it has to be mentioned that the composition of the four data blocks to one ensemble restricts the temporal homogeneity. Nevertheless, the agreement with intensity distributions, observations, and statistics is very high. In this study we have been focused on all-year variances, oscillations, or trends. Future investigations will address a seasonal differentiated analysis of trends and oscillations as well as a more detailed investigation of the spatial distribution of these findings. In particular, the simulations can be used as input for hydrological modeling and further applications such as flood risk assessments. The presented ensemble in this case acts as a stochastic weather generator treating the single simulations independently. Estimates of high return periods become more robust.

Furthermore, analyses of possible mechanisms behind observed oscillations are in preparation. Previous studies indicated that there is a strong relation between precipitation in Europe and the North Atlantic Oscillation (NAO), especially during wintertime (e.g., Hurrell, 1995; Rîmbu et al., 2002; Haylock and Goodess, 2004; Nissen et al., 2010; Pinto and Raible, 2012). Moreover, Casanueva et al. (2014) found a connection between extreme precipitation and the Atlantic Multidecadal Oscillation (AMO) during the whole year. The investigations of Bloomfield et al. (2018) revealed long-term changes in mean sea level pressure in the North Atlantic region and related storminess over Europe, which might be an artifact of a rising number of available and assimilated observations in the last decades.

*Data availability.* The E–OBS data (Haylock et al., 2008) is online available after registration at https://www.ecad.eu/download/ensembles/ensembles.php. The 20CR data (Compo et al., 2011) can be found on https://www.esrl.noaa.gov/psd/data/20thC_Rean/. HYRAS (Rauthe et al., 2013) can be requested an the German Weather Service (DWD). The RCM data (MiKlip data) will be made available via the CERA database (http://cera-www.dkrz.de/; last access: July 2019) of the German Climate Computing Center (DKRZ).

https://doi.org/10.5194/esd-2019-47
Preprint. Discussion started: 2 September 2019


Earth System Dynamics Discussions
Open Access
EGU

## Appendix A: Statistical Quantities

The Pearson correlation coefficient (Wilks, 2006) is given by

$$R = \frac{\sum_{k=1}^{N} \{[y_k - \overline{y_k}] \cdot [x_k - \overline{x_k}]\}}{\sqrt{\sum_{k=1}^{N} [x_k - \overline{x_k}]^2} \cdot \sqrt{\sum_{k=1}^{N} [y_k - \overline{y_k}]^2}} \,, \tag{A1}$$

with the data series $x$ and $y$ of length $N$. The range of $R$ is $R \in [-1; +1]$ with a perfect anti-correlation at $R = -1$ and a perfect correlation at $R = +1$.

The Gumbel distribution (Wilks, 2006) is an extreme value type-I distribution and often used for return period estimation. Its cumulative density function (cdf) is given by

$$F(x) = \exp\left(-\exp\left(-\frac{x-\beta}{\alpha}\right)\right) \,, \tag{A2}$$

with the free parameters $\beta = \sigma\sqrt{6} \cdot \pi^{-1}$ and $\alpha = \overline{x} - \gamma\beta$, where $\sigma$ is the standard deviation of the sample $x$ and $\gamma = 0.57721$ Euler's constant. For $x$ usually a series of yearly maximum values is used. The relationship between the cdf and the return period $T$ is given by (Wilks, 2006)

$$T = \frac{1}{1 - F(x)} \,. \tag{A3}$$

The signal–to–noise ration $S2N$ in this case is defined as

$$S2N = \frac{RV_{\mathrm{T,Gumbel}}}{CI_{90,\mathrm{T}}} \,, \tag{A4}$$

with the return level $RV$ of the Gumbel distribution at return period $T$ divided by the 90 % confidence interval at $T$ (Früh et al., 2010). Small values of $S2N$ indicate a more uncertain estimate, high values a more robust one.

## Appendix B: ETCCDI quantities

Two out of the 27 indices introduced and recommended by the Expert Team on Climate Change Detection and Indices[4] (ETCCDI; Karl et al., 1999; Peterson, 2005) are used in this study. R95pTOT describes the annual total precipitation sum of all values above the climatological 95 % percentile of wet days ($RR > 1$ mm) during the reference period 1961–1990. The R95pTOT of the year $k$ is defined as

$$\mathrm{R95pTOT_k} = \sum_{w=1}^{W} RR_{\mathrm{wk}} \quad \forall\, RR_{\mathrm{wk}} > RR_{\mathrm{p95}} \,, \tag{B1}$$

where $RR_{\mathrm{wk}}$ is the daily precipitation amount on a wet day during year $k$, $RR_{\mathrm{p95}}$ is the climatological 95 % percentile, and $W$ the total number of wet days in year $k$. Analogously, the R99pTOT is defined replacing the 95 % with the 99 % percentile.

$$\mathrm{R99pTOT_k} = \sum_{w=1}^{W} RR_{\mathrm{wk}} \quad \forall\, RR_{\mathrm{wk}} > RR_{\mathrm{p99}} \,. \tag{B2}$$

[4] http://etccdi.pacificclimate.org/

https://doi.org/10.5194/esd-2019-47
Preprint. Discussion started: 2 September 2019


Earth System Dynamics
Discussions
Open Access
EGU

## Appendix C: Trends and Significance

A Mann–Kendall Test (Mann, 1945; Kendall, 1955) is performed for the detection of trends and its related significance. To account for possible oscillations within long time series, we first split the complete time series into sub-series with a minimum length of 10 years and up to over 100 years (trend matrix). The Mann-Kendall Test uses a standardized test statistic $S_\tau$ following a standard Gaussian distribution (SGD). $S_\tau$ is given by:

$$S_\tau = \begin{cases} \frac{\tau-1}{\sqrt{\sigma_\tau^2}} & , \tau > 0 \, , \\ 0 & , \tau = 0 \, , \\ \frac{\tau+1}{\sqrt{\sigma_\tau^2}} & , \tau < 0 \, . \end{cases} \tag{C1}$$

Here, $\tau$ is known as the Kendall's $\tau$ and $\sigma_\tau^2$ is the variance of the standard Gaussian distribution (SGD). A detected trend is significant if $S_\tau$ lies within the upper and lower quantile $z$ of the SGD at a given significance level $\alpha$ with $S_\tau \in \left[z_{\frac{\alpha}{2}}; z_{1-\frac{\alpha}{2}}\right]$, respectively (Yue et al., 2002).

Yue et al. (2002) pointed out some weaknesses of the Mann–Kendall test in case of inherent autocorrelation. To avoid a distortion of the statistic by autocorrelation, Yue et al. (2002) presented the Trend–Free Pre–Whitening (TFPW) method. The first step is the estimation of a linear trend between two time steps $t = i$ and $t = j$ using the Theil-Sen Approach (TSA; Theil, 1950; Sen, 1968). The slope $b$ of this linear regression is given by:

$$b = median\left(\frac{x_j - x_i}{j - i}\right) \, , \forall i < j \, . \tag{C2}$$

In a second step, the original time series $x$ is detrended by subtracting $b$ at each time step $t$:

$$x'_t = x_t - b \cdot t \, . \tag{C3}$$

Afterwards, the lag-1 autocorrelation coefficient $r_1$ is removed from the trend-free series $x'$:

$$x''_t = x'_t - r_1 \cdot x'_{t-1} \, , \tag{C4}$$

where $r_1$ is given by:

$$r_1 = \frac{\frac{1}{N-1} \cdot \sum_{i=1}^{N-1} \left(x'_i - \overline{x'}\right) \cdot \left(x'_{i+1} - \overline{x'}\right)}{\frac{1}{N} \cdot \sum_{i=1}^{N} \left(x'_i - \overline{x'}\right)^2} \, . \tag{C5}$$

The modified TFPW time series $x^*$ result by re-adding the TSA-slope $b$:

$$x^*_t = x''_t + b \cdot t \, . \tag{C6}$$

This modified time series conserves the trend, but is free of autocorrelation. The Mann–Kendall Test is performed on the TFPW time series $x^*$. According to Yue et al. (2002), TFPW has to be considered in cases with non-zero TSA-slope and significant lag-1 autocorrelation. The significance of a trend or autocorrelation is tested on the 90 % ($\alpha = 0.1$), 95 % ($\alpha = 0.05$), and 99 % ($\alpha = 0.01$) significance level.

https://doi.org/10.5194/esd-2019-47
Preprint. Discussion started: 2 September 2019


Earth System Dynamics
Discussions
Open Access
EGU

*Author contributions.* FE, LAK, HF, and JGP designed the study. HF performed (parts of) the RCM simulations. LAK applied the dry–day correction. FE did the analysis and plots, and wrote the initial draft. All Authors contributed with discussions and revisions.

*Competing interests.* The authors declare that they have no conflict of interest.

*Acknowledgements.* The authors thank the National Centers for Environmental Prediction (NCEP) for providing the 20CR data. We acknowledge the E-OBS data set from the EU-FP6 project ENSEMBLES (http://ensembles-eu.metoffice.com) and the data providers in the ECA&D project (http://www.ecad.eu). We also thank the German Weather Service (DWD) for providing HYRAS. In addition, we thank the German Climate Computing Center (DKRZ, Hamburg) for computing and storage resources. We thank the BMBF for funding the MiKlip project (contract number 01LP1129A/D) and AON for funding the extreme weather events project. We acknowledge open access publishing fund of Karlsruhe Institute of Technology (KIT). Joaquim G. Pinto thanks the AXA Research Fund for support.

https://doi.org/10.5194/esd-2019-47
Preprint. Discussion started: 2 September 2019


Earth System Dynamics Discussions

## References

Berg, P., Haerter, J. O., Thejll, P., Piani, C., Hagemann, S., and Christensen, J. H.: Seasonal characteristics of the relationship between daily precipitation intensity and surface temperature, J. Geophys. Res. Atm., 114, 2009.

Berg, P., Feldmann, H., and Panitz, H.-J.: Bias correction of high resolution regional climate model data, J. Hydrol., 448-449, 80 – 92, https://doi.org/10.1016/j.jhydrol.2012.04.026, 2012.

Berg, P., Moseley, C., and Haerter, J. O.: Strong increase in convective precipitation in response to higher temperatures, Nat. Geosci., 6, 181, 2013.

Bloomfield, H. C., Shaffrey, L. C., Hodges, K. I., and Vidale, P. L.: A critical assessment of the long-term changes in the winter-time surface Arctic Oscillation and Northern Hemisphere storminess in the ERA20C reanalysis, Environ. Res. Lett., 13, 094 004, https://doi.org/10.1088/1748-9326/aad5c5, 2018.

Boer, G. J., Smith, D. M., Cassou, C., Doblas-Reyes, F., Danabasoglu, G., Kirtman, B., Kushnir, Y., Kimoto, M., Meehl, G. A., Msadek, R., Müller, W. A., Taylor, K. E., Zwiers, F., Rixen, M., Ruprich-Robert, Y., and Eade, R.: The decadal climate prediction project (DCPP) contribution to CMIP6, Geosci. Model Dev., 9, 3751–3777, https://doi.org/10.5194/gmd-9-3751-2016, 2016.

Brönnimann, S.: Weather extremes in an ensemble of historical reanalyses, in: Historical Weather Extremes in Reanalyses, pp. 7–22, Geographica Bernensia, g92 edn., https://doi.org/10.4480/GB2017.G92.01, 2017.

Brönnimann, S., Romppainen-Martius, O., Franke, J., Stickler, A. N., and Auchmann, R.: Historical weather extremes in the "Twentieth Century Reanalysis, in: Weather extremes during the past 140 years, pp. 7–17, Geographica Bernensia, g89 edn., https://doi.org/10.4480/GB2013.G89.01, 2013.

Casanueva, A., Rodríguez-Puebla, C., Frías, M. D., and González-Reviriego, N.: Variability of extreme precipitation over Europe and its relationships with teleconnection patterns, Hydrol. Earth Syst. Sci., 18, 709–725, https://doi.org/10.5194/hess-18-709-2014, 2014.

Christensen, J. H. and Christensen, O. B.: A summary of the PRUDENCE model projections of changes in European climate by the end of this century, Clim. Change, 81, 7–30, https://doi.org/10.1007/s10584-006-9210-7, 2007.

Compo, G. P., Whitaker, J. S., Sardeshmukh, P. D., Matsui, N., Allan, R. J., Yin, X., Gleason, B. E., Vose, R. S., Rutledge, G., Bessemoulin, P., Brönnimann, S., Brunet, M., Crouthamel, R. I., Grant, A. N., Groisman, P. Y., Jones, P. D., Kruk, M. C., Kruger, A. C., Marshall, G. J., Maugeri, M., Mok, H. Y., Nordli, Ø., Ross, T. F., Trigo, R. M., Wang, X. L., Woodruff, S. D., and Worley, S. J.: The twentieth century reanalysis project, Q. J. R. Meteorol. Soc., 137, 1–28, https://doi.org/10.1002/qj.776, 2011.

Dittus, A. J., Karoly, D. J., Lewis, S. C., Alexander, L. V., and Donat, M. G.: A Multiregion Model Evaluation and Attribution Study of Historical Changes in the Area Affected by Temperature and Precipitation Extremes, J. Climate, 29, 8285–8299, https://doi.org/10.1175/JCLI-D-16-0164.1, 2016.

Donat, M. G., Alexander, L. V., Herold, N., and Dittus, A. J.: Temperature and precipitation extremes in century-long gridded observations, reanalyses, and atmospheric model simulations, J. Geophys. Res. Atm., 121, 11,174–11,189, https://doi.org/10.1002/2016JD025480, 2016.

Easterling, D. R., Evans, J. L., Groisman, P. Y., Karl, T. R., Kunkel, K. E., and Ambenje, P.: Observed Variability and Trends in Extreme Climate Events: A Brief Review, Bull. Am. Meteorol. Soc., 81, 417–426, https://doi.org/10.1175/1520-0477(2000)081<0417:OVATIE>2.3.CO;2, 2000.

Ehmele, F. and Kunz, M.: Flood-related extreme precipitation in southwestern Germany: development of a two-dimensional stochastic precipitation model, Hydrol. Earth Syst. Sci., 23, 1083–1102, https://doi.org/10.5194/hess-23-1083-2019, 2019.

https://doi.org/10.5194/esd-2019-47
Preprint. Discussion started: 2 September 2019




Eyring, V., Bony, S., Meehl, G. A., Senior, C. A., Stevens, B., Stouffer, R. J., and Taylor, K. E.: Overview of the Coupled Model Intercomparison Project Phase 6 (CMIP6) experimental design and organization, Geosci. Model Dev., 9, 1937–1958, 2016.

Feldmann, H., Früh, B., Schädler, G., Panitz, H.-J., Keuler, K., Jacob, D., and Lorenz, P.: Evaluation of the precipitation for Southwestern Germany from high resolution simulations with regional climate models, Meteorol. Z., 17, 455–465, https://doi.org/10.1127/0941-2948/2008/0295, 2008.

Feldmann, H., Schädler, G., Panitz, H.-J., and Kottmeier, C.: Near future changes of extreme precipitation over complex terrain in Central Europe derived from high resolution RCM ensemble simulations, Int. J. Climatol., 33, 1964–1977, https://doi.org/10.1002/joc.3564, 2013.

Feldmann, H., Pinto, J. G., Laube, N., Uhlig, M., Moemken, J., Pasternack, A., Früh, B., Pohlmann, H., and Kottmeier, C.: Skill and Added Value of the MiKlip Regional Decadal Prediction System for Temperature over Europe, Tellus A: Dynamic Meteorology and Oceanography, 0, 0, 2019.

Feser, F., Rockel, B., von Storch, H., Winterfeldt, J., and Zahn, M.: Regional Climate Models Add Value to Global Model Data: A Review and Selected Examples, Bull. Am. Meteorol. Soc., 92, 1181–1192, https://doi.org/10.1175/2011BAMS3061.1, 2011.

Field, C. B., Barros, V., Stocker, T. F., Qin, D., Dokken, D. J., Ebi, K. L., Mastrandrea, M. D., Mach, K. J., Plattner, G.-K., Allen, S. K., Tignor, M., and Midgley, P. M. e.: Managing the Risks of Extreme Events and Disasters to Advance Climate Change Adaptation. A Special Report of Working Groups I and II of the Intergovernmental Panel on Climate Change., Cambridge University Press, Cambridge, UK, and New York, NY, USA, https://doi.org/10.1017/CBO9781139177245, 582 pp., 2012.

Früh, B., Feldmann, H., Panitz, H.-J., Schädler, G., Jacob, D., Lorenz, P., and Keuler, K.: Determination of precipitation return values in complex terrain and their evaluation, J. Climate, 23, 2257–2274, 2010.

Goovaerts, P.: Geostatistical approaches for incorporating elevation into the spatial interpolation of rainfall, J. Hydrol., 228, 113–129, https://doi.org/10.1016/S0022-1694(00)00144-X, 2000.

Hagemann, S., Loew, A., and Andersson, A.: Combined evaluation of MPI-ESM land surface water and energy fluxes, J. Adv. Model. Earth Syst., 5, 259–286, https://doi.org/10.1029/2012MS000173, 2013.

Haylock, M. R. and Goodess, C. M.: Interannual variability of European extreme winter rainfall and links with mean large-scale circulation, Int. J. Climatol., 24, 759–776, https://doi.org/10.1002/joc.1033, 2004.

Haylock, M. R., Hofstra, N., Klein Tank, A. M. G., Klok, E. J., Jones, P. D., and New, M.: A European daily high-resolution gridded data set of surface temperature and precipitation for 1950–2006, J. Geophys. Res. Atm., 113, https://doi.org/10.1029/2008JD010201, 2008.

Hirabayashi, Y., Mahendran, R., Koirala, S., Konoshima, L., Yamazaki, D., Watanabe, S., Kim, H., and Kanae, S.: Global flood risk under climate change, Nat. Clim. Change, 3, 816, https://doi.org/10.1038/nclimate1911, 2013.

Hofstra, N., Haylock, M., New, M., and Jones, P. D.: Testing E-OBS European high-resolution gridded data set of daily precipitation and surface temperature, J. Geophys. Res. Atm., 114, 2009.

Hurrell, J. W.: Decadal Trends in the North Atlantic Oscillation: Regional Temperatures and Precipitation, Science, 269, 676–679, https://doi.org/10.1126/science.269.5224.676, 1995.

Jacob, D., Petersen, J., Eggert, B., Alias, A., Christensen, O. B., Bouwer, L. M., Braun, A., Colette, A., Déqué, M., Georgievski, G., Georgopoulou, E., Gobiet, A., Menut, L., Nikulin, G., Haensler, A., Hempelmann, N., Jones, C., Keuler, K., Kovats, S., Kröner, N., Kotlarski, S., Kriegsmann, A., Martin, E., van Meijgaard, E., Moseley, C., Pfeifer, S., Preuschmann, S., Radermacher, C., Radtke, K., Rechid, D., Rounsevell, M., Samuelsson, P., Somot, S., Soussana, J.-F., Teichmann, C., Valentini, R., Vautard, R., Weber, B., and Yiou, P.: EURO-CORDEX: new high-resolution climate change projections for European impact research, Reg. Environ. Change, 14, 563–578, https://doi.org/10.1007/s10113-013-0499-2, 2014.

https://doi.org/10.5194/esd-2019-47
Preprint. Discussion started: 2 September 2019




Journel, A. G. and Huijbregts, C. J.: Mining Geostatistics, Academic press, London, 600 pp., 1978.

Jungclaus, J. H., Fischer, N., Haak, H., Lohmann, K., Marotzke, J., Matei, D., Mikolajewicz, U., Notz, D., and von Storch, J.-S.: Characteristics of the ocean simulations in MPIOM, the ocean component of the MPI-earth system model, J. Adv. Model. Earth Syst., 5, 146–172, https://doi.org/10.1002/jame.20023, 2013.

Kanamitsu, M., Alpert, J. C., Campana, K. A., Caplan, P. M., Deaven, D. G., Iredell, M., Katz, B., Pan, H.-L., Sela, J., and White, G. H.: Recent changes implemented into the global forecast system at NMC, Weather Forcast., 6, 425–435, https://doi.org/10.1175/1520-0434(1991)006%3C0425:RCIITG%3E2.0.CO;2, 1991.

Karl, T. R., Nicholls, N., and Ghazi, A.: Clivar/GCOS/WMO workshop on indices and indicators for climate extremes workshop summary, in: Weather Clim. Extrem., pp. 3–7, Springer, 1999.

Kendall, M. G.: Rank correlation methods, Charles Griffin, London, UK, 196 pp., 1955.

Kienzler, S., Pech, I., Kreibich, H., Müller, M., and Thieken, A. H.: After the extreme flood in 2002: changes in preparedness, response and recovery of flood-affected residents in Germany between 2005 and 2011, Nat. Hazards Earth Syst. Sci., 15, 505–526, https://doi.org/10.5194/nhess-15-505-2015, 2015.

Lenderink, G., Mok, H. Y., Lee, T. C., and Van Oldenborgh, G. J.: Scaling and trends of hourly precipitation extremes in two different climate zones–Hong Kong and the Netherlands, Hydrol. Earth Syst. Sci., 15, 3033–3041, 2011.

Mann, H. B.: Nonparametric Tests Against Trend, Econometrica, 13, 245–259, https://doi.org/10.2307/1907187, 1945.

Maraun, D., Wetterhall, F., Ireson, A. M., Chandler, R. E., Kendon, E. J., Widmann, M., Brienen, S., Rust, H. W., Sauter, T., Themeßl, M., Venema, V. K. C., Chun, K. P., Goodess, C. M., Jones, R. G., Onof, C., Vrac, M., and Thiele-Eich, I.: Precipitation downscaling under climate change: Recent developments to bridge the gap between dynamical models and the end user, Rev. Geophys., 48, 1–34, https://doi.org/10.1029/2009RG000314, 2010.

Marotzke, J., Müller, W. A., Vamborg, F. S. E., Becker, P., Cubasch, U., Feldmann, H., Kaspar, F., Kottmeier, C., Marini, C., Polkova, I., Prömmel, K., Rust, H. W., Stammer, D., Ulbrich, U., Kadow, C., Köhl, A., Kröger, J., Kruschke, T., Pinto, J. G., Pohlmann, H., Reyers, M., Schröder, M., Sienz, F., Timmreck, C., and Ziese, M.: MiKlip: a national research project on decadal climate prediction, Bull. Am. Meteorol. Soc., 97, 2379–2394, https://doi.org/10.1175/BAMS-D-15-00184.1, 2016.

Merz, B., Elmer, F., Kunz, M., Mühr, B., Schröter, K., and Uhlemann-Elmer, S.: The extreme flood in June 2013 in Germany, La Houille Blanche, pp. 5–10, 2014.

Mieruch, S., Feldmann, H., Schädler, G., Lenz, C.-J., Kothe, S., and Kottmeier, C.: The regional MiKlip decadal forecast ensemble for Europe: the added value of downscaling., Geosci. Model Dev., 7, https://doi.org/10.5194/gmd-7-2983-2014, 2014.

Moberg, A. and Jones, P. D.: Trends in indices for extremes in daily temperature and precipitation in central and western Europe, 1901–99, Int. J. Climatol., 25, 1149–1171, https://doi.org/10.1002/joc.1163, 2005.

Moberg, A., Jones, P. D., Lister, D., Walther, A., Brunet, M., Jacobeit, J., Alexander, L. V., Della-Marta, P. M., Luterbacher, J., Yiou, P., Chen, D., Klein Tank, A. M. G., Saladié, O., Sigró, J., Aguilar, E., Alexandersson, H., Almarza, C., Auer, I., Barriendos, M., Begert, M., Bergström, H., Böhm, R., Butler, C. J., Caesar, J., Drebs, A., Founda, D., Gerstengarbe, F.-W., Micela, G., Maugeri, M., Österle, H., Pandzic, K., Petrakis, M., Srnec, L., Tolasz, R., Tuomenvirta, H., Werner, P. C., Linderholm, H., Philipp, A., Wanner, H., and Xoplaki, E.: Indices for daily temperature and precipitation extremes in Europe analyzed for the period 1901–2000, J. Geophys. Res. Atm., 111, https://doi.org/10.1029/2006JD007103, 2006.

https://doi.org/10.5194/esd-2019-47
Preprint. Discussion started: 2 September 2019




Moorthi, S., Pan, H.-L., and Caplan, P.: Changes to the 2001 NCEP operational MRF/AVN global analysis/forecast system, in: Technical Procedures Bulletin 484, US Department of Commerce, National Oceanic and Atmospheric Administration, National Weather Service, Office of Meteorology, Program and Plans Division, 2001.

Mudelsee, M., Börngen, M., Tetzlaff, G., and Grünewald, U.: No upward trends in the occurrence of extreme floods in central Europe, Nature, 425, 166, https://doi.org/10.1038/nature01928, 2003.

Mudelsee, M., Börngen, M., Tetzlaff, G., and Grünewald, U.: Extreme floods in central Europe over the past 500 years: Role of cyclone pathway "Zugstrasse Vb", J. Geophys. Res. Atm., 109, https://doi.org/10.1029/2004JD005034, 2004.

Mueller, W. A., Pohlmann, H., Sienz, F., and Smith, D.: Decadal climate predictions for the period 1901–2010 with a coupled climate model, Geophys. Res. Lett., 41, 2100–2107, https://doi.org/10.1002/2014GL059259, 2014.

Müller, W. A., Baehr, J., Haak, H., Jungclaus, J. H., Kröger, J., Matei, D., Notz, D., Pohlmann, H., von Storch, J. S., and Marotzke, J.: Forecast skill of multi-year seasonal means in the decadal prediction system of the Max Planck Institute for Meteorology, Geophys. Res. Lett., 39, https://doi.org/10.1029/2012GL053326, 2012.

Müller, W. A., Jungclaus, J. H., Mauritsen, T., Baehr, J., Bittner, M., Budich, R., Bunzel, F., Esch, M., Ghosh, R., Haak, H., Ilyina, T., Kleine, T., Kornblueh, L., Li, H., Modali, K., Pohlmann, H., Roeckner, E., Stemmler, I., Tian, F., and Marotzke, J.: A Higher-resolution Version of the Max Planck Institute Earth System Model (MPI-ESM1. 2-HR), J. Adv. Model. Earth Syst., 10, 1383–1413, https://doi.org/10.1029/2017MS001217, 2018.

MunichRe: NatCatSERVICE, natcatservice.munichre.com/, accessed: 23 Aug 2018, 2017.

Nissen, K. M., Leckebusch, G. C., Pinto, J. G., Renggli, D., Ulbrich, S., and Ulbrich, U.: Cyclones causing wind storms in the Mediterranean: characteristics, trends and links to large-scale patterns, Nat. Hazards Earth Syst. Sci., 10, 1379–1391, https://doi.org/10.5194/nhess-10-1379-2010, 2010.

Nissen, K. M., Ulbrich, U., and Leckebusch, G. C.: Vb cyclones and associated rainfall extremes over Central Europe under present day and climate change conditions, Meteorol. Z., 22, 649–660, https://doi.org/10.1127/0941-2948/2013/0514, 2013.

O'Gorman, P. A.: Precipitation extremes under climate change, Current climate change reports, 1, 49–59, 2015.

Pauling, A. and Paeth, H.: On the variability of return periods of European winter precipitation extremes over the last three centuries, Clim. Past., 3, 65–76, https://doi.org/10.5194/cp-3-65-2007, 2007.

Peleg, N., Fatichi, S., Paschalis, A., Molnar, P., and Burlando, P.: An advanced stochastic weather generator for simulating 2-D high-resolution climate variables, J. Adv. Model. Earth Sy., 9, 1595–1627, https://doi.org/10.1002/2016MS000854, 2017.

Peterson, T. C.: Climate change indices, WMO Bull., 54, 83–86, 2005.

Pinto, J. G. and Raible, C. C.: Past and recent changes in the North Atlantic oscillation, WIRES Clim Change, 3, 79–90, https://doi.org/10.1002/wcc.150, 2012.

Poli, P., Hersbach, H., Dee, D. P., Berrisford, P., Simmons, A. J., Vitart, F., Laloyaux, P., Tan, D. G. H., Peubey, C., Thépaut, J.-N., Trémolet, Y., Hólm, E. V., Bonavita, M., Isaksen, L., and Fisher, M.: ERA-20C: An atmospheric reanalysis of the twentieth century, J. Climate, 29, 4083–4097, https://doi.org/10.1175/JCLI-D-15-0556.1, 2016.

Rauthe, M., Steiner, H., Riediger, U., Mazurkiewicz, A., and Gratzki, A.: A Central European precipitation climatology - Part I: Generation and validation of a high-resolution gridded daily data set (HYRAS), Meteorol. Z., 22, 235–256, https://doi.org/10.1127/0941-2948/2013/0436, 2013.

Reyers, M., Feldmann, H., Mieruch, S., Pinto, J. G., Uhlig, M., Ahrens, B., Früh, B., Modali, K., Laube, N., Moemken, J., Müller, W., Schädler, G., and Kottmeier, C.: Development and prospects of the regional MiKlip decadal prediction system over Europe: predictive



skill, added value of regionalization, and ensemble size dependency, Earth Syst. Dynam., 10, 171–187, https://doi.org/10.5194/esd-10-171-2019, 2019.

Rhodes, R. I., Shaffrey, L. C., and Gray, S. L.: Can reanalyses represent extreme precipitation over England and Wales?, Q. J. R. Meteorol. Soc., 141, 1114–1120, https://doi.org/10.1002/qj.2418, 2015.

Rîmbu, N., Boroneanţ, C., Buţă, C., and Dima, M.: Decadal variability of the Danube river flow in the lower basin and its relation with the North Atlantic Oscillation, International Journal of Climatology, 22, 1169–1179, https://doi.org/10.1002/joc.788, 2002.

Rockel, B., Will, A., and Hense, A.: The regional climate model COSMO-CLM (CCLM), Meteorol. Z., 17, 347–348, https://doi.org/10.1127/0941-2948/2008/0309, 2008.

Schewe, J., Gosling, S. N., Reyer, C., Zhao, F., Ciais, P., Elliott, J., Francois, L., Huber, V., Lotze, H. K., Seneviratne, S. I., van Vliet, M. T. H., Vautard, R., Wada, Y., Breuer, L., Büchner, M., Carozza, D. A., Chang, J., Coll, M., Deryng, D., de Wit, A., Eddy, T. D., Folberth, C., Frieler, K., Friend, A. D., Gerten, D., Gudmundsson, L., Hanasaki, N., Ito, A., Khabarov, N., Kim, H., Lawrence, P., Morfopoulos, C., Müller, C., Müller Schmied, H., Orth, R., Ostberg, S., Pokhrel, Y., Pugh, T. A. M., Sakurai, G., Satoh, Y., Schmid, E., Stacke, T., Steenbeek, J., Steinkamp, J., Tang, Q., Tian, H., Tittensor, D. P., Volkholz, J., Wang, X., and Warszawski, L.: State-of-the-art global models underestimate impacts from climate extremes, Nature communications, 10, 1005, https://doi.org/10.1038/s41467-019-08745-6, 2019.

Schröter, K., Kunz, M., Elmer, F., Mühr, B., and Merz, B.: What made the June 2013 flood in Germany an exceptional event? A hydro-meteorological evaluation, Hydrol. Earth Syst. Sci., 19, 309–327, https://doi.org/10.5194/hess-19-309-2015, 2015.

Sen, P. K.: Estimates of the Regression Coefficient Based on Kendall's Tau, J. Am. Stat. Assoc., 63, 1379–1389, https://doi.org/10.1080/01621459.1968.10480934, 1968.

Singer, M. B., Michaelides, K., and Hobley, D. E. J.: STORM 1.0: a simple, flexible, and parsimonious stochastic rainfall generator for simulating climate and climate change, Geosci. Model Dev., 11, 3713–3726, 2018.

Stephens, G. L. and Ellis, T. D.: Controls of global-mean precipitation increases in global warming GCM experiments, J. Climate, 21, 6141–6155, 2008.

Stevens, B., Giorgetta, M., Esch, M., Mauritsen, T., Crueger, T., Rast, S., Salzmann, M., Schmidt, H., Bader, J., Block, K., Brokopf, R., Fast, I., Kinne, S., Kornblueh, L., Lohmann, U., Pincus, R., Reichler, T., and Roeckner, E.: Atmospheric component of the MPI-M earth system model: ECHAM6, J. Adv. Model Earth Syst., 5, 422–446, https://doi.org/10.1002/jame.20015, 2013.

Stucki, P., Rickli, R., Brönnimann, S., Martius, O., Wanner, H., Grebner, D., and Luterbacher, J.: Weather patterns and hydro-climatological precursors of extreme floods in Switzerland since 1868, Meteorol. Z., 21, 531–550, https://doi.org/10.1127/0941-2948/2012/368, 2012.

Stucki, P., Dierer, S., Welker, C., Gómez-Navarro, J. J., Raible, C. C., Martius, O., and Brönnimann, S.: Evaluation of downscaled wind speeds and parameterised gusts for recent and historical windstorms in Switzerland, Tellus A: Dynamic Meteorology and Oceanography, 68, 31 820, https://doi.org/10.3402/tellusa.v68.31820, 2016.

Taylor, K. E., Stouffer, R. J., and Meehl, G. A.: An overview of CMIP5 and the experiment design, Bull. Am. Meteorol. Soc., 93, 485–498, https://doi.org/10.1175/BAMS-D-11-00094.1, 2012.

Theil, H.: A rank-invariant method of linear and polynomial regression analysis, Proceedings of the Royal Netherlands Academy of Sciences, 53, Part I: 386–392, Part II:521–525, Part III: 1397–1412, https://doi.org/10.1007/978-94-011-2546-8_20, 1950.

Toreti, A., Xoplaki, E., Maraun, D., Kuglitsch, F.-G., Wanner, H., and Luterbacher, J.: Characterisation of extreme winter precipitation in Mediterranean coastal sites and associated anomalous atmospheric circulation patterns, Nat. Hazards Earth Syst. Sci., 10, 1037–1050, https://doi.org/10.5194/nhess-10-1037-2010, 2010.

https://doi.org/10.5194/esd-2019-47
Preprint. Discussion started: 2 September 2019




Torma, C., Giorgi, F., and Coppola, E.: Added value of regional climate modeling over areas characterized by complex terrain–Precipitation over the Alps, J. Geophys. Res. Atm., 120, 3957–3972, https://doi.org/10.1002/2014JD022781, 2015.

Trenberth, K. E., Dai, A., Rasmussen, R. M., and Parsons, D. B.: The changing character of precipitation, Bull. Am. Meteorol. Soc., 84, 1205–1218, 2003.

Uhlemann, S., Thieken, A. H., and Merz, B.: A consistent set of trans-basin floods in Germany between 1952-2002, Hydrol. Earth Syst. Sci., 14, 1277, https://doi.org/10.5194/hess-14-1277-2010, 2010.

Ulbrich, U., Brücher, T., Fink, A. H., Leckebusch, G. C., Krüger, A., and Pinto, J. G.: The central European floods of August 2002: Part 1 – Rainfall periods and flood development, Weather, 58, 371–377, https://doi.org/10.1256/wea.61.03A, 2003a.

Ulbrich, U., Brücher, T., Fink, A. H., Leckebusch, G. C., Krüger, A., and Pinto, J. G.: The central European floods of August 2002: Part 2 –Synoptic causes and considerations with respect to climatic change, Weather, 58, 434–442, https://doi.org/10.1256/wea.61.03B, 2003b.

van den Besselaar, E. J. M., Haylock, M. R., van der Schrier, G., and Klein Tank, A. M. G.: A European daily high-resolution observational gridded data set of sea level pressure, J. Geophys. Res. Atm., 116, https://doi.org/10.1029/2010JD015468, 2011.

Westra, S., Alexander, L. V., and Zwiers, F. W.: Global increasing trends in annual maximum daily precipitation, J. Climate, 26, 3904–3918, 2013.

Wilks, D. S.: Statistical Methods in the Atmospheric Sciences, vol. 91 of *International Geophysics Series*, Academie Press, San Diego, California, USA, 2nd edn., 2006.

Yue, S., Pilon, P., Phinney, B., and Cavadias, G.: The influence of autocorrelation on the ability to detect trend in hydrological series, Hydrol. Process., 16, 1807–1829, https://doi.org/10.1002/hyp.1095, 2002.

Zolina, O., Simmer, C., Kapala, A., Bachner, S., Gulev, S., and Maechel, H.: Seasonally dependent changes of precipitation extremes over Germany since 1950 from a very dense observational network, J. Geophys. Res. Atm., 113, https://doi.org/10.1029/2007JD008393, 2008.

Zwiers, F. W., Alexander, L. V., Hegerl, G. C., Knutson, T. R., Kossin, J. P., Naveau, P., Nicholls, N., Schär, C., Seneviratne, S. I., and Zhang, X.: Climate extremes: challenges in estimating and understanding recent changes in the frequency and intensity of extreme climate and weather events, in: Climate Science for Serving Society, pp. 339–389, Springer, 2013.